

UNIVERSITY OF CALIFORNIA,  
IRVINE

Studies of the O-Demethylation of Guaiacols by Acetogenic Gut Bacteria and Discovery of a  
Gut Bacterial Gene that is Sufficient to Activate the Phytoestrogen Enterolactone

THESIS

submitted in partial satisfaction of the requirements  
for the degree of

MASTER OF SCIENCE

in Chemistry

by

Barry E. Rich

Thesis Committee:  
Assistant Professor Elizabeth N. Bess, Chair  
Professor Jennifer A. Prescher  
Distinguished Professor James S. Nowick

2021

© Jayme C. Jackson  
© 2021 Lizett Ortiz de Ora  
© 2021 Zane G. Long  
© Kylie S. Uyeda  
© 2021 Paola Nol Bernardino  
© 2021 Elizabeth N. Bess  
© 2021 Barry E. Rich

## **DEDICATION**

I dedicate this work to my brother and favorite actor, Eric F. Rich, as well as to my sisters and parents.

I also dedicate this work to my Dungeons & Dragons group. Our weekly adventures were a great source of ongoing joy during the production of this work. As with our scientific work, the story does not truly end. It is simply a matter of “Where last we left our heroes...”

# TABLE OF CONTENTS

	Page
LIST OF FIGURES	iv
ACKNOWLEDGEMENTS	v
ABSTRACT OF THE THESIS	vi
INTRODUCTION	1
CHAPTER 1: Dopamine Production by Acetogenic Gut Bacteria that O-Demethylate 3-Methoxytyramine, a Metabolite of Catechol O-Methyltransferase	3
CHAPTER 2: Expanding the Breadth of Methoxyarenes O-Demethylated by Acetogenic Gut Bacteria	21
CHAPTER 3: Identifying Gut Bacterial Gene Required for Enterolactone Formation	28
CHAPTER 4: Summary and Conclusions	34
REFERENCES	35
APPENDIX A: Supplementary Figures	40

## LIST OF FIGURES

		Page
Figure 1.1	Interactions between Gut Bacteria and Dopamine Metabolism	5
Figure 1.2	Degradation of 3-Methoxytyramine to Dopamine by Fecal Bacteria	12
Figure 1.3	Degradation of 3-Methoxytyramine to Dopamine by Gut Bacterial Isolates	13
Figure 1.4	Inhibition of 3-Methoxytyramine O-Demethylation by Propyl Iodide	15
Figure 1.5	Increased Acetate Production by Gut Bacteria Exposed to 3-Methoxytyramine	16
Figure 2.1	O-Demethylation of Guaiacol Panel by Gut Bacterial Isolates	25
Figure 2.2	Potential Interactions between Gut Bacterial and Estrogen Metabolism	25
Figure 3.1	Enterolactone Production by Gut Bacterial Consortium	29
Figure 3.2	Production of Enterolactone Encoded by <i>edl2</i>	32

## ACKNOWLEDGEMENTS

I would like to express thanks for my committee chair, Professor Elizabeth N. Bess, for her guidance throughout the course of my graduate studies, as well as to my committee members, Professor Jennifer A. Prescher and Professor James S. Nowick, for their feedback and perspective during both my advancement exam and the preparation of this thesis.

I would also like to express my gratitude to Dr. Lizett Ortiz de Ora, Jayme C. Jackson, Zane G. Long, Kylie S. Uyeda, Yasmine Alam, Paola Nol Bernardino, Kimberly Ly, Orla Hannon, Michael Faryab, Christina Xu, and Brianna Robbins for being such wonderful colleagues and lab mates over the years.

I am indebted to Dr. Felix Grun for technical assistance and consultation in the development of mass spectrometry assays.

I wish to thank Separation Research (Turku, Finland) for donating hydroxymatairesinol to the Bess Lab. This unexpected gift was incredibly useful in quickly resolving an issue that arose with an LC-MS/MS assay.

Financial support was provided by the University of California, Irvine, University of California, Irvine American Chemical Society Institutional Research Grant (IRG-16-187-13), and an Achievement Rewards for College Scientists (ARCS) Foundation Scholar Award.

The data and methods presented in Chapter 3 were previously published in *Nature Microbiology*, a Springer Nature Journal, and is presented here with permission (CC-BY, Creative Commons Attribution 4.0 International License).

The following figures were created using BioRender: Figure 1.1 (agreement number RX2311G12H), Figure 1.2 (agreement number US2311BDRL), Figure 1.3 (agreement number CH230YOOY0), Figure 1.4 (agreement number HU2311UO31), Figure 1.5 (agreement number HR2311YSN5), Figure S1 (agreement number WA2311WUVP), and Figure S2 (agreement number RM230WHLCE).

## ABSTRACT OF THE THESIS

Studies of the O-Demethylation of Guaiacols by Acetogenic Gut Bacteria and Discovery of a Gut Bacterial Gene that is Sufficient to Activate the Phytoestrogen Enterolactone

by

Barry E. Rich

Master of Science in Chemistry

University of California, Irvine, 2021

Assistant Professor Elizabeth N. Bess, Chair

The gut microbiome contributes to the overall metabolism of numerous compounds that circulate in and out of the gastrointestinal tract, including endogenous, dietary, and pharmaceutical molecules. Herein, three projects are presented aimed at uncovering bacterial species and genes responsible for the chemistry carried out by the gut microbiome. In the first, a previously unreported route for the production of dopamine by gut bacteria is posed. Dopamine, which is abundant in the gut, is converted to 3-methoxytyramine (3MT) by the human enzyme catechol *O*-methyltransferase (COMT). Communities of fecal bacteria are demonstrated to *O*-demethylate 3MT to produce dopamine. Two prominent acetogens found in the GI tract, *Eubacterium limosum* and *Blautia producta*, are shown to carry out this metabolism. This metabolism is shown to likely be carried out by cobalamin-dependent methyltransferases, as metabolism is reversibly inhibited by propyl iodide. In the second, I identify additional guaiacol metabolites that *E. limosum* and *B. producta* can *O*-demethylate to their respective guaiacols: vanillylmandelic acid, 3-*O*-methyldopa, and 2-methoxyestradiol. In the third, I determined that the gut bacterial protein called enterodiol lactonizing enzyme (Edl) is sufficient for converting enterodiol (END)—produced by gut bacterial metabolism of diet-derived molecules—into the phytoestrogen enterolactone (ENL). ENL has been reported to have anti-breast cancer effects in rodent models and humans. Thus, an absence of the bacterial genes

required to produce ENL in an individual's gut microbiome may serve as a biomarker for an increased risk for breast cancer.



## INTRODUCTION

The gut microbiome—comprising trillions of bacteria harbored within the gastrointestinal (GI) tract—is increasingly recognized as an important factor in human health and disease.<sup>1</sup> Each individual has a unique gut microbiome, shaped over the course of their life by one's diet, pharmaceutical exposure, and environmental factors.<sup>2</sup> Variation in gut microbiome composition, in terms of the abundance of different taxa, has been noted as a possible factor in human health and disease. For a variety of diseases, including but not limited to Parkinson's disease, Crohn's disease, and breast cancer, it has been found that patients and non-patients have significantly different gut microbiome compositions.<sup>3–5</sup> Substantial progress has been made in the field to determine the impact of the gut microbiome on disease; however, we overwhelmingly do not yet know the chemical level mechanisms by which the gut microbiome impacts human health and disease.

The gut microbiome has the potential to influence human health and disease through a wide array of metabolic actions. The GI tract is a high traffic environment through which dietary, pharmaceutical, and endogenous compounds come into contact with gut bacteria. Harbored within gut bacteria are millions of genes which allow for them to modify molecules passing through the GI tract in ways that human cells cannot. While the functions of many of these genes remain to be characterized, it has already been demonstrated that their presence has substantial consequences for the host.<sup>6</sup> Understanding the chemical means by which gut bacteria impact the host is crucial for elucidating the role of the gut microbiome in maintaining human health and assessing disease risk.

In this thesis, I present three projects centered on identifying the chemical mechanisms by which the gut microbiome impacts human health and disease. In the first, I present research investigating a novel role that gut bacteria might play in regulating the metabolism of dopamine, an abundant hormone within the GI tract that plays a crucial role in gut motility. In the second, I

examine the ability of gut bacteria to O-demethylate a panel of guaiacols (compounds containing the 2-methoxyphenol motif) comprising dietary, pharmaceutical, and endogenous compounds. In the third, I identify a gene in the gut bacteria *Lactonifactor longoviformis* that is sufficient for the production of the phytoestrogen enterolactone as part of a gut bacterial consortium.

# **CHAPTER 1: Dopamine Production by Acetogenic Gut Bacteria that O-Demethylate 3-Methoxytyramine, a Metabolite of Catechol O- Methyltransferase**

Hormone levels are tuned in the body through ways that we are only beginning to understand. There is accumulating evidence that a key piece of this metabolism puzzle is the gut microbiota, which encodes for millions of diverse biochemical reactions that remain largely uncharacterized. Robust differences in the levels of several hormones have been detected in rodents based on whether the intestine is colonized with bacteria or entirely devoid of these microorganisms (i.e., germ-free).<sup>7</sup> Additionally, variations in the collections of bacteria that compose the gut microbiota are correlated with changes in circulating levels of hormones, including serotonin and estrogens.<sup>5,8,9</sup> The sources of such hormone changes remain incompletely defined, although there is evidence that the gut microbiota can impact hormone levels in two ways: bacterial regulation of hormone production by the host<sup>10</sup> and synthesis of these endocrine molecules by gut bacteria.<sup>11,12</sup> Here, we present a previously unexamined route for gut bacterial dopamine synthesis, which the gut microbiota may use to dictate levels of dopamine *in vivo*.

Dopamine, although most widely known for its neurotransmitter role, is a potent hormone that is present in the bloodstream at varying levels across people.<sup>13</sup> One route by which dopamine enters the bloodstream is following its absorption from the intestine,<sup>14</sup> a body site harboring nearly half of peripheral dopamine (i.e., dopamine outside the brain).<sup>15</sup> There is evidence that the gut microbiota is a significant variable in control of peripheral dopamine levels: colonizing germ-free mice with a murine gut microbiota resulted in over a two-fold increase in dopamine levels in the colonic lumen.<sup>16</sup> Although peripheral dopamine has significant and diverse biological effects that include modulating blood pressure, insulin levels, metabolic

disease, and gastrointestinal (GI) motility, the precise bacteria and their biochemical pathways that modulate dopamine levels remain poorly understood.<sup>17–20</sup>

One route by which gut bacteria can contribute to dopamine production is through biotransformation of small molecules that are endogenous to the host. Gut bacteria *Enterococcus faecalis* and *Enterococcus faecium* produce dopamine by decarboxylating levodopa (L-dopa), an anti-Parkinsonian drug, via a tyrosine decarboxylase (TyrDC) (**Fig. 1.1**).<sup>21,22</sup> L-Dopa may be produced from tyrosine, as fecal metagenomes encode for tyrosinase homologs, which are enzymes that convert tyrosine to L-dopa;<sup>23</sup> however, the biochemical activities of these homologs in gut bacteria remain to be functionally characterized. There is evidence that intestinal dopamine may also derive from gut bacterial hydrolysis of dopamine glucuronides,<sup>16</sup> which are metabolites formed in a variety of tissues, including the liver and intestine.<sup>24</sup> Several gut bacteria have also been reported to synthesize dopamine from undefined culture media,<sup>25</sup> but the molecular precursors and the biochemical pathways that they traverse to be converted to dopamine remain incompletely characterized.

Here, we examine whether gut bacteria have the metabolic potential to elevate intestinal dopamine levels by counteracting host mechanisms for dopamine regulation. Peripheral dopamine levels are regulated by catechol O-methyltransferase (COMT).<sup>26</sup> This enzyme, which is highly expressed in the liver and GI tract,<sup>27</sup> methylates dopamine to the aryl methyl ether 3-methoxytyramine (3MT) (**Fig. 1.1**). There are several examples of gut bacteria O-demethylating aryl methyl ethers,<sup>28–31</sup> although gut bacterial O-demethylation of 3MT has remained unexamined. Studies in rats suggest that the gut microbiota can counteract COMT's regulation of dopamine levels *in vivo*. In rats intraperitoneally dosed with <sup>14</sup>C-labeled 3-O-methyldopa (the metabolite afforded by COMT O-methylation of L-dopa), demethylation of 3-O-methyldopa only occurred once this compound was excreted in bile to the GI tract; no demethylation occurred in rats with fistula that prevented biliary excretion.<sup>32</sup> These findings indicate that 3-O-methyldopa,

which is structurally analogous to 3MT, is *O*-demethylated *in vivo*, but only upon entering the GI tract.

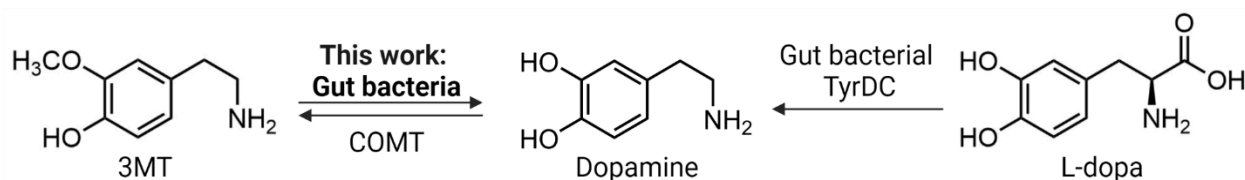


**Figure 1.1** Dopamine can be *O*-methylated to 3-methoxytyramine (3MT) by catechol *O*-methyltransferase (COMT); this biotransformation attenuates the dopaminergic properties of dopamine. In this work, we identify that gut bacteria have the metabolic potential to counteract COMT's metabolism of dopamine by *O*-demethylating 3MT. Gut bacteria have previously been characterized to synthesize dopamine by decarboxylating levodopa (L-dopa) using tyrosine decarboxylase (TyrDC).

The GI lumen is a putative reservoir of 3MT, owing to 3MT being naturally present in the fecal excreta of rats.<sup>33,34</sup> Within the gut microbiome, 3MT is in the midst of gut bacteria that are capable of *O*-demethylating a diverse array of molecules that also harbor the aryl methyl ether motif.<sup>28–30,35</sup> Such *O*-demethylation is commonly carried out by acetogens.<sup>30,36,37</sup> These bacteria use cobalamin-dependent enzymes to funnel the methyl group of aryl methyl ethers into production of acetate through a process called reductive acetogenesis.<sup>38,39</sup> Several gut bacterial acetogens have been functionally characterized to demethylate dietary aryl methyl ethers<sup>40–43</sup> and encode genetic homologs for aryl methyl ether-dependent reductive acetogenesis.<sup>39,44,45</sup> These gut bacteria include *Eubacterium limosum*<sup>29</sup> and *Blautia producta*,<sup>30</sup> which are members of the dominant gut microbiota (10<sup>8</sup> CFUs per gram of feces).<sup>31</sup> Here, we report the ability of *E. limosum* and *B. producta* to produce dopamine via the *O*-demethylation of 3MT. Furthermore, our findings provide supporting evidence for the involvement of cobalamin-dependent methyltransferases in the reversion of 3MT to dopamine.

## MATERIALS AND METHODS

### Materials:

*Blautia producta* (DSM 2950 and DSM 3507) and *Eubacterium limosum* DSM 20543 were cultured in Brain Heart Infusion (BHI, Difco) supplemented with 0.05% w/v L-cysteine HCl

(BHI+C). Bacteria were cultured in anoxic conditions (2–5% H<sub>2</sub>, 20% CO<sub>2</sub>, with the balance being N<sub>2</sub>) in a Coy Anaerobic Chamber. Experiments assessing the growth inhibition of conversion of 3MT to dopamine by propyl iodide and the production of acetate were performed in an acetogenic media (defined below). Fecal samples were cultured in Gifu Anaerobic Broth (GAM, Fisher Scientific). Media was equilibrated in anoxic conditions overnight to remove oxygen.

Chemicals were sourced as follows: 3-methoxytyramine HCl (3MT, 99%+, Acros Organics, 172851000), dopamine HCl (Alfa Aesar, AAA1113606), isoproterenol HCl (Cayman Chemical Company, 15592), methanol (HPLC Grade. Avantor/J.T. Baker), acetonitrile (LiChrosolv, Millipore Sigma), propyl iodide (99%, Sigma-Aldrich, 171883, and hexanes (HPLC Grade, Fisher Chemical).

Media and components for media were sourced as follows: brain heart infusion (BD Difco), brain heart infusion Agar (BD Difco, DF0418-17-7), Gifu anaerobic broth (GAM, Fisher Scientific, M1801), vitamin supplement, 100X (MD-VS, ATCC), D-glucose anhydrous (VWR Life Science, Biotechnology Grade), phosphate-buffered saline (10X) pH 7.4 (Thermo Fisher Scientific, 70011044), sodium bicarbonate (Sigma-Aldrich, S6014), L-cysteine HCl (Fisher Scientific, BP376), and casamino acids (Fisher Scientific DF0288-15-6).

Acetogenic media was prepared to contain the following: 5 mM glucose, 0.2% casamino acids, 0.2% sodium bicarbonate, 1X ATCC vitamins, 22 mM PBS, and 0.05% L-cysteine HCl in basal media. Basal media was prepared to contain the following: 1X Pfennig and Lippert trace elements, 116 nM sodium selenite, 136 nM sodium tungstate, 230 mM ammonium chloride, 2 mM calcium chloride, 2 mM magnesium sulfate, and 34 mM sodium chloride in double-deionized water. 333X Pfennig and Lippert trace elements were prepared to contain the following: 17 mM ethylenediaminetetraacetic acid, 8.4 mM iron (II) sulfate, 348 μM zinc sulfate, 152 μM manganese chloride, 4.9 mM boric acid, 841 μM cobalt (II) chloride, 58 μM copper (II)

chloride, 77  $\mu\text{M}$  nickel chloride, 82  $\mu\text{M}$  sodium molybdate in double-deionized water adjusted to pH 4.0.

#### Fecal studies:

Fecal samples were obtained from seven healthy humans. All subjects consented to participate in the study, which was approved by the University of California, Irvine Institutional Review Board. Subjects self-reported as being in good health and were screened to exclude subjects with gastrointestinal illnesses, bacterial infections, chronic viral infections, and sexually transmitted diseases, as well as subjects engaging in intravenous drug use. Fecal samples were introduced into an anaerobic chamber, and each was resuspended in pre-reduced phosphate buffer saline (PBS), pH 7.4 at a final concentration of 0.1 g/mL. Suspensions were vortexed for 5 minutes and then allowed to settle for 5 min. The fecal slurries were diluted 1:100 into Gifu anaerobic media (GAM) supplemented with 3MT (500  $\mu\text{M}$  in sterile double-deionized water) or vehicle control. The cultures were anaerobically cultured at 37 °C for 72 hrs. Quantification of 3MT and dopamine was conducted using the LC–MS/MS assay described below.

#### Incubations of bacteria with 3MT *in vitro*:

Incubations with gut bacteria were carried out in brain heart infusion supplemented with 0.05% w/v L-cysteine HCl. Seed cultures were grown overnight in triplicate in anoxic conditions (2–5%  $\text{H}_2$ , 20%  $\text{CO}_2$ , with the balance being  $\text{N}_2$ ) at 37 °C. Seed cultures were normalized to an  $\text{OD}_{600}$  of 0.5 in fresh media, then diluted 1:100 into media that was subsequently supplemented with 3MT (500  $\mu\text{M}$  in sterile double-deionized water) or an equal amount of its vehicle. Cultures were incubated at 37 °C for 72 hours in triplicate with sterile controls. After 72 hours, samples were removed from the anaerobic chamber and centrifuged at 2000 RPM for 20 minutes at 4

°C. Supernatant (50 µL) was diluted five-fold in 0.2% L-ascorbic acid in water and immediately frozen at -20 °C until analyzed using LC–MS/MS.

#### Light-reversible inhibition of 3MT O-demethylation by propyl iodide:

Incubations with *E. limosum* DSM 20543 and *B. producta* DSM 3507 were carried out in acetogenic media. Seed cultures were grown overnight in triplicate in brain heart infusion supplemented with 0.05% w/v L-cysteine HCl and in anoxic conditions (2–5% H<sub>2</sub>, 20% CO<sub>2</sub>, with the balance being N<sub>2</sub>) at 37 °C. Seed cultures were normalized to an OD<sub>600</sub> of 0.5 in fresh acetogenic media, then diluted 1:100 into acetogenic media that was subsequently supplemented with 3MT (500 µM in double-deionized water) and either propyl iodide (20 µM in ethanol) or an equivalent volume of vehicle (ethanol). Two sets of each media type were prepared in triplicate with sterile controls. Both sets of incubations containing 3MT and propyl iodide and one set of incubations containing 3MT and propyl iodide's vehicle were wrapped in aluminum foil to block out light; the fourth culture containing 3MT and propyl iodide's vehicle was exposed to light. Growth was tracked by measuring OD<sub>600</sub>, and 100 µL aliquots of culture were sampled periodically over the course of incubation to assess metabolism of 3MT to dopamine. Aliquots were centrifuged at 2000 RPM for 10 minutes at 4 °C, and 50 µL of supernatant was diluted five-fold in 0.2% w/v L-ascorbic acid<sub>(aq.)</sub>. Samples were then immediately frozen at -20 °C to preserve for analysis using LC–MS/MS. After reaching mid- to late-logarithmic phase of growth, one set of cultures containing 3MT and propyl iodide and another set with 3MT but without propyl iodide were exposed to light using a 60-Watt incandescent light bulb at a distance of no greater than 10 cm. Light exposure was maintained for the duration of the incubation.

#### Quantification of 3MT and dopamine by LC–MS/MS:



Concentrations of 3MT and dopamine from incubations of gut bacteria with 3MT were assessed by electrospray ionization (ESI) triple-quadrupole liquid chromatography–spectrometry (LC–MS/MS, Acquity UPLC and Quattro Premier XE; Waters Micromass) in positive-ion mode with single reaction monitoring. Solvent A was 0.2% acetic acid and 1.8% acetonitrile in water, while solvent B was 0.2% acetic acid in acetonitrile. The concentration of solvent B was 10–90% from 0–2 min, 90–10% from 2–3 min, and 10% for 3–4 min. The column temperature was 50 °C. A C18 column (Acquity UPLC BEH; 1.7 µM; 2.1 mm × 50 mm; Waters part number 186002350) was used. The injection volume was 10 µL. Retention times were as follows: 3MT, 0.79 min; dopamine, 0.76 min; isoproterenol, 0.83 min. The capillary voltage was 4.00 kV and the cone voltage was 10V, with a source temperature of 125 °C. The desolvation gas flow was 800 L h<sup>-1</sup> and the desolvation temperature was 400 °C. The [M–H]<sup>+</sup> *m/z* values of parent/daughter ions were as follows: 3MT, 167.86/151.03; dopamine, 153.85/137.03; isoproterenol, 212.10/193.90.

Stock solutions of 3MT and dopamine were prepared at 50 mM in 0.2% L-ascorbic acid<sub>(aq.)</sub>. These were used to generate a standard containing 3MT and dopamine (each standard at 1 mM in either brain heart infusion media (for screening bacteria for metabolism) or in acetogenic media (for assessing the inhibition of metabolism by propyl iodide)). These 1 mM standard solutions were serially diluted two-fold in their respective sterile media to 244 nM. Each standard (50 µL) was then diluted two-fold into isoproterenol (50 µM in 0.2% L-ascorbic acid<sub>(aq.)</sub>). Standards were further diluted ten-fold in methanol, chilled at -80 °C for 15 minutes, and centrifuged at 10000xg, 4 °C for 10 minutes to precipitate proteins. Supernatant (50 µL) was diluted ten-fold in 10% acetonitrile in water. The calibration curve ranges used for quantification were 4.9 nM to 5 µM for 3MT and 20 nM to 5 µM for dopamine, with a limit of quantification set at a signal-to-noise ratio of 10:1. Calibration curves were generated by measuring peak areas and performing linear regression against known concentrations.

Supernatant (50  $\mu$ L) from incubations was diluted five-fold in 0.2% L-ascorbic acid and immediately frozen at -20  $^{\circ}$ C to preserve samples for LC–MS/MS. After thawing, preserved supernatant (50  $\mu$ L) from incubations with 3MT were diluted two-fold into isoproterenol (50  $\mu$ M in 0.2% L-ascorbic acid<sub>(aq.)</sub>). Next, samples were diluted ten-fold in methanol, chilled at -80  $^{\circ}$ C for 15 minutes, and centrifuged at 10000xg, 4  $^{\circ}$ C for 10 minutes to precipitate proteins. Supernatant (50  $\mu$ L) was diluted ten-fold in 10% acetonitrile in water, and injected into the LC–MS/MS instrument. Dopamine and 3MT concentrations were quantified using calibration curves.

#### Quantification of acetate, propionate, and butyrate by GC–MS:

Short-chain fatty acid concentrations (acetate, propionate, and butyrate) were quantified through a GC–MS method adapted from S. Kage *et. al.*<sup>46</sup> All concentrations for short-chain fatty acids are reported relative to the sterile media used to construct the calibration curve.

Acetate, propionate, and butyrate from incubations of bacterial isolates were derivatized with pentafluorobenzyl bromide, and their concentrations were assessed by positive-ion electron ionization (EI+) single-quadrupole gas chromatography–mass spectrometry (TRACE™ GC ULTRA and ISQ; Thermo-Fisher Scientific). Samples were run on a TG-SQC column (15 m x 0.25 mm x 0.25  $\mu$ M). Oven temperature was initially set at 40  $^{\circ}$ C with a 20  $^{\circ}$ C/min ramp to 290  $^{\circ}$ C. Retention times of the short-chain fatty acid derivatives were as follows: pentafluorobenzyl acetate, 6.734 min; pentafluorobenzyl propionate, 7.425 min; pentafluorobenzyl butyrate, 8.054 min; ethyl phenylacetate (internal standard), 8.024 min. The [M–H]<sup>+</sup> *m/z* values for the pentafluorobenzyl fragment (*m/z* = 181.05) of each derivative were used to quantify each acid derivative. Ethyl phenylacetate was quantified using the benzyl fragment peak (*m/z* = 91.09). Signal for each derivative was calculated as a ratio to the ethyl phenylacetate internal standard signal, (i.e., response for quantitation).

Stock solutions of sodium acetate, sodium propionate, and sodium butyrate were prepared at 1 M in double-deionized water. These were used to generate a standard containing

acetate, propionate, and butyrate at 200 mM in double-deionized water, which was subsequently serially diluted, two-fold, to create standards ranging from 50 mM to 49  $\mu$ M in double-deionized water. To 50  $\mu$ L of each standard were added 50  $\mu$ L of sterile media, 100  $\mu$ L of a solution containing both ethyl phenylacetate (5 mM) and pentafluorophenol (5 mM) in sodium phosphate<sub>(aq)</sub> (500 mM, pH 6.8), followed by 200  $\mu$ L of pentafluorobenzyl bromide (500 mM in acetone). Standards were vortexed to mix and incubated at 60 °C for 1.5 hours with shaking at 1000 RPM. Standards were then centrifuged at 10000xg for 1 minute. To each standard, 1000  $\mu$ L of hexanes were added, vortexed for 15 seconds to extract, and centrifuged at 10000xg for 1 minute. Then, 100  $\mu$ L of extract was diluted ten-fold in hexanes and transferred to GC–MS vials for analysis. The calibration curve ranges used for quantification were 98  $\mu$ M to 12.5 mM for acetate, propionate, and butyrate, with a limit of quantification set at a signal-to-noise ratio of 10:1. Calibration curves were generated by measuring peak areas and performing linear regression against known concentrations. Pentafluorophenol did not end up being used in the quantification process.

To 50  $\mu$ L of whole-cell culture from samples were added 50  $\mu$ L of double-deionized water, 100  $\mu$ L of a solution containing both ethyl phenylacetate (5 mM) and pentafluorophenol (5 mM) in sodium phosphate<sub>(aq)</sub> (500 mM, pH 6.8), followed by 200  $\mu$ L of pentafluorobenzyl bromide (500 mM in acetone). Samples were vortexed to mix and incubated at 60 °C for 1.5 hours with shaking at 1000 RPM. Samples were then centrifuged at 10000xg for 1 minute. To each sample, 1000  $\mu$ L of hexanes were added, vortexed for 15 seconds to extract, and centrifuged at 10000xg for 1 minute. Then, 100  $\mu$ L of extract was diluted ten-fold in hexanes and transferred to GC–MS vials for analysis.

#### Assessment of growth advantage via 3MT supplementation:

Seed cultures of gut bacteria were grown overnight in triplicate in brain heart infusion supplemented with 0.05% w/v L-cysteine HCl in anoxic conditions (2–5% H<sub>2</sub>, 20% CO<sub>2</sub>, with the

balance being N<sub>2</sub>) at 37 °C. Seed cultures were normalized to an OD<sub>600</sub> of 0.5 in acetogenic media, then diluted 1:100 into acetogenic media supplemented with 3MT (1 mM or 0.1 mM in sterile double-deionized water) or equal amounts of its vehicle. Cultures were incubated at 37 °C for 38 hours in triplicate with sterile controls. Growth was monitored by OD<sub>600</sub> in 15-minute intervals with 30 seconds of shaking at 500 RPM prior to each spectrophotometric reading.

## RESULTS

### **3MT is reverted to dopamine by communities of fecal bacteria:**

In order to assess whether gut bacteria are capable of *O*-demethylating 3MT, fecal samples collected from healthy human donors (n = 7) were anaerobically incubated with 3MT

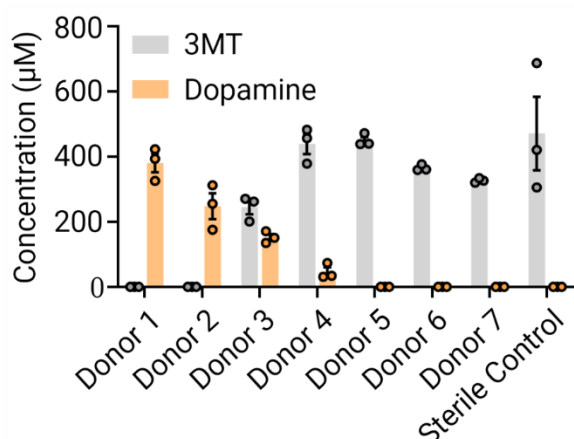


**Figure 1.2.** Fecal samples from healthy human donor (n = 7) were cultured with 3MT (500 μM) or vehicle. Dopamine and 3MT were quantified using LC–MS/MS. No dopamine was detectable in vehicle controls for any donor. (n = 3 technical replicates; bars are mean ± SEM).

(500 μM) or vehicle in nutrient-rich media. In cultures of fecal samples from four of seven donors, 3MT was degraded to dopamine (**Fig. 1.2**). These data indicate that gut bacteria can revert 3MT to the active hormone, dopamine, but that this metabolic capacity may vary across people. Incubations of fecal samples from two donors (Donors 1 and 2) resulted in complete consumption of 3MT, whereas only 51% of 3MT was consumed by Donor 3 and 12% by Donor 4.

In these cultures, dopamine production was similarly detected at varying levels. Dopamine was not produced in any vehicle control from any donor, suggesting that the observed production of dopamine was a result of 3MT *O*-demethylation. In cultures of Donors 1 and 2, a substoichiometric quantity of dopamine formed, despite 3MT being completely consumed; the amount of dopamine produced relative to 3MT consumed was 76% and 50%, respectively. The unaccounted-for metabolic fate of 3MT may be due to dopamine degradation,

which can be carried out by some gut bacteria.<sup>47</sup> Taken together, our data show that fecal bacterial communities are capable of reverting 3MT to dopamine, although the occurrence of this metabolic capacity as well as the extent of metabolism likely varies across individuals.

**Gut bacterial acetogens *E. limosum* and *B. producta* produce dopamine by O-demethylating 3MT:**

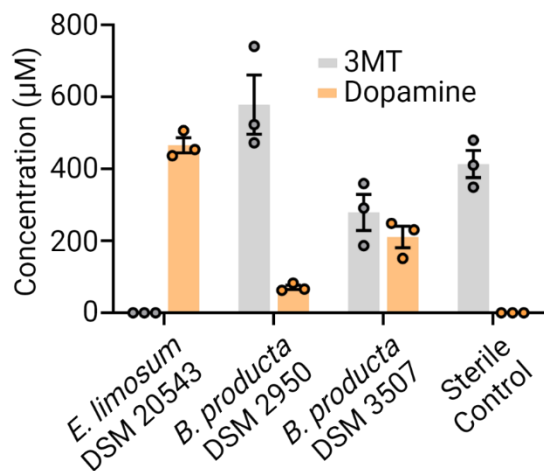


**Figure 1.3.** *E. limosum* and *B. producta* were incubated with 3MT (500 µM) for 72 hours, at which point O-demethylation was quantified by LC–MS/MS. (n = 3 biological replicates; bars are mean ± SEM).

Seeking to identify members of the gut microbiota that may be responsible for the O-demethylation of 3MT, we focused on two prominent acetogenic gut bacteria, *Eubacterium limosum* and *Blautia producta*, that are known to O-demethylate dietary aryl methyl ethers.<sup>29,42,43</sup>

Additionally, two strains of *B. producta* were screened to assess possible strain-level variation in 3MT metabolism. *E. limosum* DSM 20543 and *B. producta* DSM 2950 and DSM 3507 were

anaerobically cultured with 3MT (500 µM) or vehicle in nutrient-rich media. Following incubation, concentrations of 3MT and dopamine were assessed using LC–MS/MS (**Fig. 1.3**). *E. limosum* DSM 20543 quantitatively converted 3MT to dopamine. Likewise, both strains of *B. producta* converted 3MT to dopamine, although to a lesser extent: DSM 2950 converted 14% of 3MT to dopamine and 42% of 3MT was converted to dopamine by DSM 3507.

**Conversion of 3MT to dopamine is likely performed by a cobalamin-dependent methyltransferase:**

Having identified prominent members of the gut microbiota that are capable of degrading 3MT to dopamine, we endeavored to identify the cellular machinery responsible for this transformation. Literature precedent indicates that O-demethylation of aryl methyl ethers by

acetogens, including *E. limosum* and *B. producta*, is carried out by cobalamin-dependent methyltransferases.<sup>43,48</sup> These enzymes can be inhibited by propyl iodide, and inhibition is reversed by photolysis.<sup>49</sup> To determine whether 3MT O-demethylation is performed by cobalamin-dependent enzymes, we tested whether this biotransformation could be inhibited by propyl iodide and, subsequently, rescued by light.

*E. limosum* DSM 20543 and *B. producta* DSM 3507 were each cultured in acetogenic media with 3MT (500  $\mu$ M) as well as propyl iodide (20  $\mu$ M) or vehicle. As propyl iodide inhibition of cobalamin-dependent methyltransferases is sensitive to light, bacteria were initially cultured in the dark and subsequently exposed to light. Growth was monitored by OD<sub>600</sub>, and O-demethylation was periodically assessed using LC–MS/MS. Neither propyl iodide nor light significantly impacted growth of *E. limosum* DSM 20543 (**Fig. 1.4A**) or *B. producta* DSM 3507 (**Fig. 1.4B**). In the absence of light, O-demethylation of 3MT by *E. limosum* DSM 20543 was completely inhibited by propyl iodide (**Fig. 1.4C**). For *B. producta* DSM 3507, 83% of 3MT O-demethylation was inhibited at 15 hours relative to cultures not exposed to propyl iodide (**Fig. 1.4D**). Upon exposing cultures with propyl iodide to light, *E. limosum* DSM 20543 regained the ability to O-demethylate 3MT, affording a 2.4-fold increase (at 24 hours) in dopamine concentration relative to cultures that were maintained in the dark; for *B. producta*, a 1.8-fold

increase in dopamine concentration was observed upon exposure of cultures to light (at 17 hours). The light-reversible inhibitory effects of propyl iodide suggest that cobalamin-dependent methyltransferases in both *E. limosum* DSM 20543 and *B. producta* DSM 3507 are responsible for the O-demethylation of 3MT to form dopamine.

**3MT Drives Increases in Acetate Production by *E. limosum* and *B. producta*:**

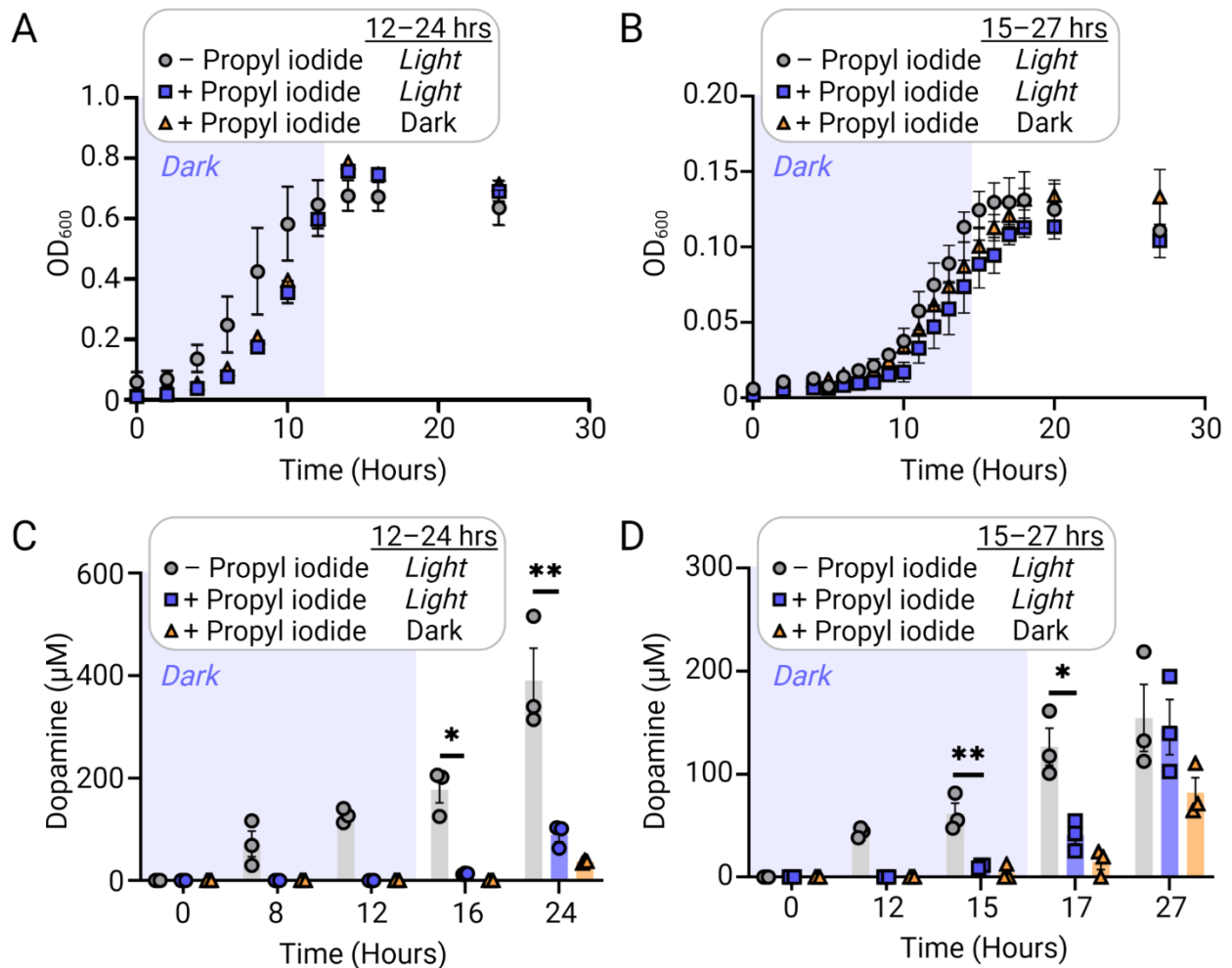


**Figure 1.4.** (A) *E. limosum* DSM 20543 and (B) *B. producta* DSM 3507 were each anaerobically cultured with 3MT (500 μM) as a function of propyl iodide (20 μM) and light exposure. Growth was measured using the optical density of cultures at 600 nm (OD<sub>600</sub>). Cultures were maintained in the dark from 0–12 hours (*E. limosum* DSM 20543) or 0–15 hours (*B. producta* DSM 3507). Next, cultures without propyl iodide and half of the cultures with propyl iodide were exposed to light. Cultures of (C) *E. limosum* DSM 20543 and (D) *B. producta* DSM 3507 were periodically sampled, and dopamine production was measured by LC–MS/MS. (n = 3 biological replicates; values/bars are mean ± SEM; significance was determined by 1-way ANOVA; \*, P ≤ 0.05, \*\*, P ≤ 0.01).

Owing to the reported abilities of bacterial acetogens to use aryl methyl ethers as a carbon source for acetate synthesis,<sup>39,44,45</sup> we sought to determine whether the demethylation of 3MT to dopamine could drive acetate production. *E. limosum* DSM 20543 as well as *B. producta* strains DSM 2950 and DSM 3507 were each cultured in the presence of 3MT (2 mM) or vehicle and in a medium designed to promote acetogenesis.<sup>50</sup> Concentrations of short-chain fatty acids acetate, propionate, and butyrate were quantified through a GC–MS method adapted from S.

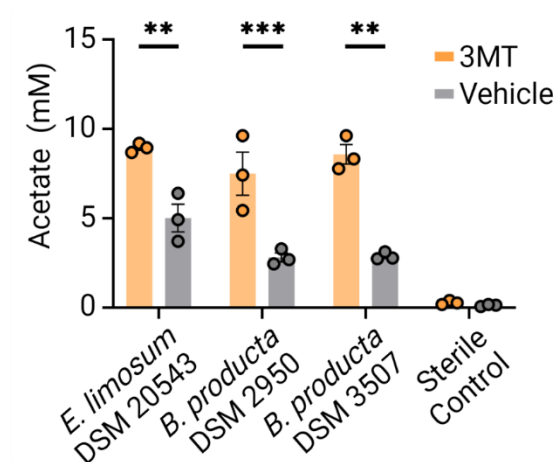


**Figure 1.5.** *E. limosum* DSM 20543 as well as the *B. producta* strains DSM 2950 and DSM 3507 were each cultured in acetogenic media with 3MT (2 mM) or its vehicle. Acetate levels were quantified using GC–MS. (n = 3 biological replicates; bars are mean ± SEM; significance was determined by unpaired *t*-test; \*\*:  $P \leq 0.006$ ; \*\*\*:  $P = 0.0002$ ).

Kage *et. al.*<sup>46</sup> For all strains tested, acetate levels were significantly higher in cultures incubated with 3MT as compared to vehicle (**Fig. 1.5**).

Measures of propionate (**Fig. S1A**) and butyrate (**Fig. S1B**) did not differ between treated and vehicle groups, which suggests that the acetate produced is not coming from fermentation, where increases in each of these short-chain fatty acids would be expected. It has been reported that *E. limosum* and *B. producta*, as well as other

acetogens, are sometimes capable of deriving a growth advantage from certain aryl methyl ethers.<sup>36</sup> A preliminary assessment to determine if *B. producta* could derive a growth advantage from 3MT was conducted; however, no growth advantage was detected (**Fig. S2**).

## DISCUSSION

Our data suggest the existence of a novel way that affords gut bacteria the potential to regulate dopamine levels. This gut bacterial metabolism entails formation of dopamine by *O*-demethylation of 3MT, which is a metabolite endogenously produced by COMT to attenuate dopamine levels.<sup>51</sup> Conversion of 3MT to dopamine was observed in incubations with fecal bacteria from four of seven different donors. This variability is likely due to differences in gut



bacterial species as well as strains of species that exist across people. Towards elucidating a source of this variability, we sought to identify specific gut bacteria that can mediate 3MT O-demethylation. Because other aryl methyl ethers are O-demethylated by gut bacterial acetogens *E. limosum* and *B. producta*,<sup>42,43,52</sup> we tested the abilities of these organisms to O-demethylate 3MT. While both of these bacterial species were capable of converting 3MT to dopamine, the extent of conversion differed between both of the two species tested as well as the two strains of *B. producta* examined. *E. limosum* DSM 20543 completely metabolized 3MT, while the two *B. producta* strains only partially metabolized 3MT. Furthermore, of the two strains of *B. producta* tested, DSM 3507 metabolized significantly more 3MT than did DSM 2950. Determining whether these differences in extent of 3MT metabolism are biologically significant or artifacts of *in vitro* culturing requires characterization of both the enzymes responsible for this process as well as the occurrence of this biochemical process *in vivo*.

Discovering the biochemical origin of the 3MT O-demethylation pathway will enable assessment of this pathway's contribution to dopamine levels in GI tracts harboring a complex gut microbiota. To begin this process, we set out to determine the class of enzyme responsible for O-demethylating 3MT. Prior studies in other organisms determined that cobalamin-dependent methyltransferases O-demethylate aryl methyl ethers<sup>53</sup> and that this process is inhibited by propyl iodide in a light-reversible fashion.<sup>54</sup> Cobalamin-dependent methyltransferases operate by transferring the methyl abstracted from the aryl methyl ether to the cobalt center of the cobalamin cofactor. Then, cobalamin relays the methyl to a methyl acceptor, which in this system is tetrahydrofolate.<sup>55</sup> When cobalamin-dependent methyltransferases are exposed to propyl iodide, the result is a cobalt–propyl bond where the propyl group is not transferred to tetrahydrofolate, impairing further O-demethylation.<sup>49</sup> Although the cobalt–propyl bond cannot be biochemically cleaved, this bond is photolyzed, which reverses inhibition of O-demethylation.<sup>49</sup>

Owing to *E. limosum* and *B. producta* encoding several putative cobalamin-dependent methyltransferases,<sup>39,44,45,53</sup> we used propyl iodide as a diagnostic for whether 3MT is O-demethylated by members of this enzyme class. Our studies exposing *E. limosum* DSM 20543 as well as the *B. producta* strains DSM 3507 and DSM 2950 to propyl iodide, in the absence of light, demonstrated that 3MT O-demethylation was inhibited by propyl iodide. Importantly, propyl iodide had no significant impact on bacterial growth, indicating that the observed metabolic inhibition was not due to a growth defect but likely due to inhibition of a cobalamin-dependent methyltransferase. Moreover, exposing cultures to light partially reversed inhibition, further diagnostic of a cobalamin-dependent methyltransferase mediating the conversion of 3MT to dopamine. Identifying the specific gene and enzyme responsible for this biotransformation of 3MT is the subject of ongoing work in our laboratory and will be critical to determining the contribution of 3MT O-demethylation to inter-individual differences in dopamine metabolism in the GI tract.

Bacterial acetogens that O-demethylate aryl methyl ethers using cobalamin-dependent methyltransferases have been reported to funnel both the methyl group of this substrate and CO<sub>2</sub> into the synthesis of acetate through a process called reductive acetogenesis.<sup>38,39</sup> Owing to *E. limosum* and *B. producta* each being capable of reductive acetogenesis,<sup>56,57</sup> we suspected that these bacteria may use 3MT to produce acetate. Indeed, 3MT drove significant increases in the acetate produced by *E. limosum* DSM 20543 and both *B. producta* strains when each was cultured using acetogenic media that contained 3MT and glucose as the sole carbon sources. Concentrations of propionate and butyrate, other short-chain fatty acids that are abundantly produced by gut bacteria,<sup>58,59</sup> were not impacted by the presence of 3MT. These data suggest that the unique increase in acetate was not due to 3MT inducing a generalized increase in short-chain fatty acid synthesis. Curiously, we observed a supra-stoichiometric increase in acetate concentration relative to the amount of 3MT supplied. This could mean that 3MT induces an alternative pathway for reductive acetogenesis, perhaps the canonical route in which

CO<sub>2</sub> and H<sub>2</sub> are coupled to produce acetate.<sup>60–62</sup> Previous reports indicate that acetogens can incorporate the methyl group obtained from aryl methyl ethers into acetate.<sup>38</sup> Not all of the acetate produced in this experiment could have been synthesized that way. However, the question remains as to whether the increased acetate production is a result of 3MT O-demethylation and an alternative process such as reductive acetogenesis, or simply that alternative process. Additional experimentation is necessary to answer this question. Regardless, the reported role of cobalamin-dependent enzymes in producing acetate from aryl methyl ethers combined with our findings that 3MT enhances acetate production provides further support for 3MT O-demethylation being performed by a cobalamin-dependent methyltransferase. These findings also provide motivation for investigating secondary metabolites that are exposed to and metabolized by the gut microbiota that may serve as undiscovered regulators of gut bacterial central metabolism.

It remains necessary to examine the *in vivo* relevance of 3MT O-demethylation to the regulation of dopamine levels. The biogeography of 3MT-to-dopamine metabolism is likely critical to whether this process contributes to variation in blood dopamine levels. Whether dopamine produced in the GI tract by 3MT O-demethylation may reenter the systemic circulation requires further study *in vivo*. Regardless, dopamine produced from 3MT O-demethylation may have impacts within the GI tract, where dopamine regulates gut motility.<sup>63</sup>

## CONCLUSION

Our data demonstrate that the gut microbiota, both bacterial isolates and fecal bacterial communities, are capable of O-demethylating dopaminergic metabolites *in vitro*. Here, we identified two prominent members of the gut microbiota, *E. limosum* and *B. producta*, that can revert 3MT to dopamine. Additional studies provided supporting evidence that the degradation of 3MT to dopamine is carried out by cobalamin-dependent methyltransferases in these species. Taken together, our findings point to a new pathway by which the gut microbiota might

impact dopamine metabolism in the GI tract. If operative *in vivo*, gut bacterial 3MT O-demethylation to form dopamine would counteract a process by which the host attenuates levels of dopamine through its O-methylation to 3MT. The balance between host methylation of dopamine to form 3MT and bacterial O-demethylation of 3MT to form dopamine may be significant to the regulation of dopamine levels outside the brain. Such alterations to peripheral dopamine metabolism could have profound impacts on host health. Consequently, these *in vitro* findings motivate further studies to assess the occurrence of 3MT-to-dopamine metabolism *in vivo* and the potential impacts of this metabolic process on the host.

## CHAPTER 2: Expanding the Breadth of Methoxyarenes O-Demethylated by Acetogenic Gut Bacteria

The chief focus of my studies was on the O-demethylation of 3MT by dopamine (Chapter 1); however, there are a variety of guaiacols that are part of the chemical environment of the GI tract. These come from endogenous sources, such as 3MT, as well as dietary sources. However, the scope of guaiacols that are O-demethylated and the bacteria responsible for this metabolism remain unknown, as do the genes that encode for this function.<sup>37,38,42,43</sup> This gap in knowledge limits our understanding of how this metabolism affects community composition in the gut microbiome and the effect of gut microbial metabolism on the regulation of bioactive catechols by the host.

A multi-pronged approach was undertaken to identify both the guaiacols that the gut microbiome can O-demethylate and the responsible bacterial species. These include *in vitro* screenings of biologically relevant guaiacols with gut bacterial isolates of species previously reported to perform O-demethylation in order to identify the breadth of O-demethylation. Additionally, a two-pronged approach to selectively culture O-demethylating bacteria from the complex communities found within human stool was pursued. These approaches capitalized on the resistance to select antibiotics and acetogenic characteristics of methoxyarene metabolizers. These strategies complement each other in order to discover the scope of both guaiacols that are O-demethylated and the bacterial species responsible for the observed metabolism.

### MATERIALS AND METHODS

#### Materials:

Homovanillic acid (HVA), 3,4-dihydroxyphenylacetic acid (DOPAC), 3-O-methyldopa and levodopa (L-dopa) were obtained from Oakwood Chemicals. Dexamethasone, vanillylmandelic acid (VMA), and dopamine HCl were obtained from Alfa Aesar. From Carbosynth, 3,4-

dihydroxymandelic acid was obtained. 2-hydroxyestradiol (2-HE<sub>2</sub>) and (2-ME<sub>2</sub>) were obtained from Toronto Research Chemicals. All chemicals were ≥95% pure. Ethyl acetate (+99.5% for spectroscopy) used in extractions was purchased from Acros Organics. Acetonitrile (LiChrosolv®) and acetone (LiChrosolv®) used for LC–MS/MS sample preparation were purchased from Millipore Sigma.

#### Incubations with guaiacols *in vitro*:

Incubations with gut bacteria were carried out in brain heart infusion supplemented with 0.05% w/v L-cysteine HCl. Seed cultures were grown overnight in triplicate in anoxic conditions (2–5% H<sub>2</sub>, 20% CO<sub>2</sub>, with the balance being N<sub>2</sub>) at 37 °C. Seed cultures were normalized to an OD<sub>600</sub> of 0.5 in fresh media, then diluted 1:100 into media that was subsequently supplemented with either HVA, VMA, 3-OMD (500 μM in sterile double-deionized water), or 2-ME<sub>2</sub> (10 μM in methanol) or an equal amount of their respective vehicles. Incubations were carried out in anoxic conditions at 37 °C for 48 hours, after which point cells were pelleted and supernatant was extracted. Samples to be analyzed by Arnow test were immediately prepared, as described below. Samples to be analyzed by LC-MS/MS were diluted 5-fold in 0.2% w/v L-ascorbic acid in double-deionized water in 96-well PCR plates to prevent oxidation, sealed with aluminum foil, and stored at -20 °C until analysis.

#### Analysis of catechol production by Arnow's Test:

A standard curve for 3-OMD, L-dopa, HVA, DOPAC, VMA, and DHMA were prepared as follows. From a 50 mM stock solution, a 1.28 mM standard was prepared in a 96-well plate. A 2-fold serial dilution was carried out on each solution to create standards from 1.28 mM to 20 μM with final volumes of 100 μL. Volumes were then adjusted to 25 μL. Then, 25 μL of supernatant was transferred to the same 96-well plate. The following reagents were added sequentially with mixing by aspiration and ejection: 25 μL 0.5 M HCl<sub>(aq)</sub>, 25 μL 1 mg/mL NaNO<sub>2</sub>:Na<sub>2</sub>MoO<sub>4(aq)</sub>, and 25 μL 1

M NaOH<sub>(aq)</sub>. The absorbance was then read at 500 nM in a plate reader (Spectrostar Nano, BMG Lab Technologies).

#### Quantification of 2-ME<sub>2</sub> and 2-HE<sub>2</sub> by LC-MS/MS:

Concentrations of 2-HE<sub>2</sub> and 2-ME<sub>2</sub> from incubation experiments were assessed by electrospray ionization (ESI) triple-quadrupole liquid chromatography mass spectrometry (Acquity UPLC and Quattro Premier XE; Waters Micromass) in positive-ion mode with single-reaction monitoring. Solvent A was 0.2% v/v acetic acid<sub>(aq)</sub> and solvent B was 0.2% v/v acetic acid in acetonitrile. The concentration of solvent B was 10–90% from 0–4 min. The temperature was 50 °C. A C18 Column (Acquity UPLC BEH; 1.7 µM; 2.1 mm × 50 mm; Waters part number 186002350) was used. The injection volume was 10 µL. Retention times were as follows: 2-HE<sub>2</sub> = 2.56 min, 2-ME<sub>2</sub> = 2.26 min, and dexamethasone (DEX) = 0.83 min which was used as an internal standard. The capillary voltage was 3.30 kV and the cone voltage was 10 V, with a source temperature of 125 °C. The desolvation gas flow was 800 l h<sup>-1</sup> and the desolvation temperature was 400 °C. The [M-H]<sup>-</sup>m/z values of parent/daughter ions were as follows: 2-HE<sub>2</sub> = 755.3/170; 2-ME<sub>2</sub> = 536.2/171; and DEX = 393.0/373.0. Working stocks of 2-HE<sub>2</sub> and 2-ME<sub>2</sub> were prepared at 50 µM (prepared from 1 mM stocks in methanol) in BHI+C with 0.2% L-ascorbic acid (prepared from 10% w/v L-ascorbic acid in ddH<sub>2</sub>O). From this, a solution with 5 µM of 2-HE<sub>2</sub> and 2-ME<sub>2</sub> was prepared in BHI+C with 0.2% L-ascorbic acid. Then, 2-fold serial dilutions were carried out to create standards from 5 µM to 2.5 nM in BHI+C with 0.2% L-ascorbic acid at final volumes of 200 µL. This was diluted two-fold into 4 µM of dexamethasone (DEX) in 0.2% L-ascorbic acid<sub>(aq)</sub> (prepared from a 10 mM stock in methanol that was used to create a working stock of 500 µM in 0.2% L-ascorbic acid<sub>(aq)</sub>) to create a final volume of 200 µL. This afforded a final standard curve of 2.5 µM to 1.25 nM of E<sub>2</sub>, 2-HE<sub>2</sub>, and 2-ME<sub>2</sub> with an internal standard of DEX at 2 µM. Samples were thawed and similarly diluted two-fold into 4 µM DEX to create a final volume of 200 µL. Standards and samples were extracted twice with ethyl acetate, the organic layer of which was removed and dried by centrifugal vacuum

concentration (Refrigerated CentriVap Concentrator (Labconco part number 7310020) and DryFast Ultra (Welch part number 20422B-01)). Samples were resuspended in 100  $\mu$ L 0.1 M  $\text{NaHCO}_3$  buffer (pH = 9) and 100  $\mu$ L of 1 mg/mL dansyl chloride in acetone, vortexed for 30 sec and heated in a water bath at 60 °C for 5 min. Reaction mixtures were then transferred to mass spectrometry vials and immediately analyzed.

## RESULTS

### Colorimetric screening of guaiacols for *in vitro* metabolism by gut bacterial acetogens:

A preliminary panel of four guaiacol substrates were screened against *E. limosum* and *B. producta*, as are known to perform *O*-demethylation. The guaiacols initially screened were endogenous metabolites of two human hormones and a pharmaceutical: vanillylmandelic acid (VMA, human metabolite of norepinephrine), homovanillic acid (HVA, human metabolite of dopamine), and 3-*O*-methyldopa (3-OMD, the COMT-inactivated guaiacol of the anti-Parkinsonian drug L-dopa). For the purposes of initial screening, a colorimetric assay called the Arnow test<sup>64</sup> to detect the production of catechols (**Fig. 2.1A**) from a panel of guaiacols (**Fig. 2.1B**). None of the strains assessed were shown to produce the catechol 3,4-dihydroxymandelic acid (DHMA) from VMA, but all were found to convert 3-OMD to L-dopa. Additionally, *B. producta* DSM 3507 was able to convert HVA to its respective catechol, 3,4-dihydroxymandelic acid (DOPAC) (**Fig. 2.1C**). This provides useful preliminary information as to the differential ability of gut bacteria



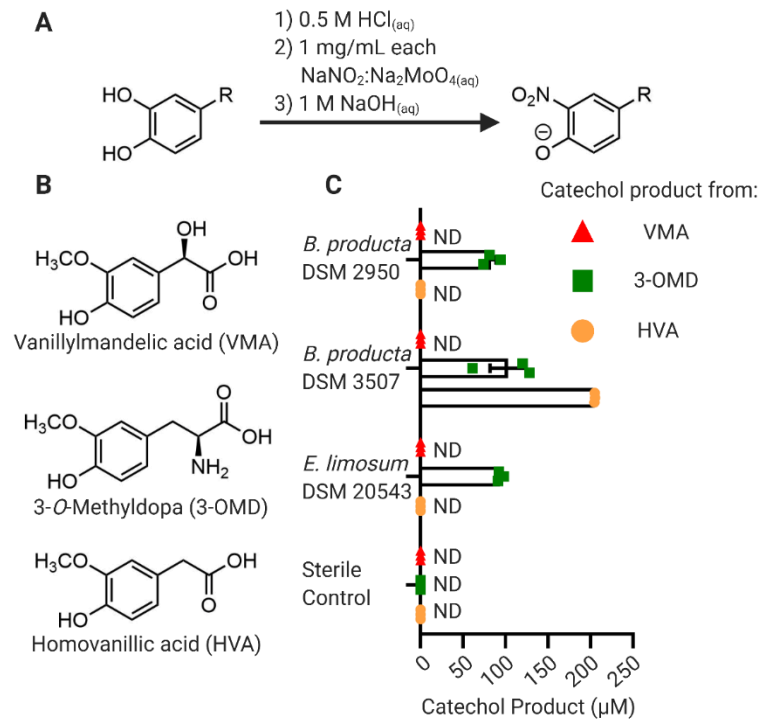


**Fig. 2.1** A) The Arnow test detects catechols by converting them to nitrophenolates, which absorb light strongly at 500 nm. B) Structures of the guaiacols VMA, HVA, and 3-OMD and their respective catechols. C) Production of catechols produced by the O-demethylation of VMA, 3-OMD, and HVA by *B. producta* DSM 2950, *B. producta* DSM 3507, and *E. limosum* DSM 20543 as measured by the Arnow test. Incubations carried out at 500 µM for all compounds. Bars represent mean ± SEM, n = 3 biological triplicates. ND = below limit of detection.

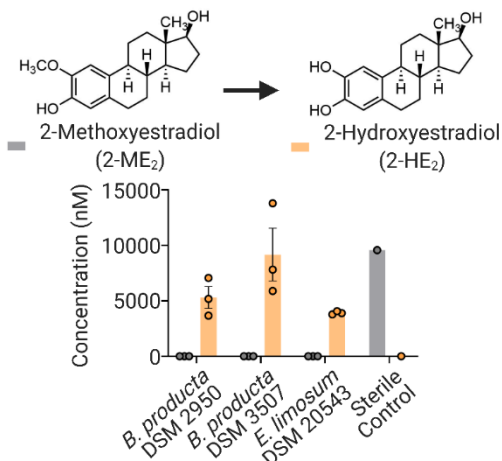


**Fig. 2.2** Incubations with 2ME<sub>2</sub> (10 µM) show it is O-demethylated to form 2-HE<sub>2</sub> by *B. producta* strains DSM 2950 and DSM 3507, as shown by LC-MS/MS. Bars are mean ± SEM, n=3 biological replicates.

to O-demethylate different guaiacols. This is evinced by the fact that *B. producta* 3507 is able to O-demethylate HVA but not VMA, which differs only by having a benzylic alcohol.

Metabolism of estrogen metabolite in vitro by gut bacterial acetogens:

In the meantime, a LC-MS/MS assay was used to screen demethylation of additional guaiacols, specifically 2-methoxyestradiol (2-ME<sub>2</sub>). Estradiol is metabolized in the liver, where it is hydroxylated by cytochrome P450s

to form 2-hydroxyestradiol (2-HE<sub>2</sub>) which is then converted to 2-ME<sub>2</sub> by COMT before being excreted to the gut.<sup>15</sup> Using an LC-MS/MS assay developed by my colleague Paola Nol Bernardino, I discovered that *E. limosum* DSM 20543 and *B. producta* DSM 2950 and *B. producta* DSM 3507 convert 2-ME<sub>2</sub> to 2-HE<sub>2</sub> in vitro (Fig. 2.2). It had previously been reported that methoxyestrogens were demethylated by a bacterial consortium from human stool;<sup>15</sup> however, the specific bacterial species responsible,

amongst the hundreds present in the bacterial consortium, had remained unknown. Identification of bacteria that encode this metabolism could provide an explanation for the observed variability in estrogen metabolites and a molecular basis for understanding the relationship between levels of estrogen metabolites and breast cancer risk.<sup>65</sup> Although no 2-ME<sub>2</sub> was detected following incubation with *B. producta*, only a fraction of the amount of possible 2-HE<sub>2</sub> that could be produced from the provided 2-ME<sub>2</sub> was detected: 40% in *E. limosum* and 50% in *B. producta* DSM 2950. Additional metabolic activity may account for the missing mass balance.

## DISCUSSION

Initial screens to identify which guaiacolic substrates can be O-demethylated by gut bacterial acetogens combined both a colorimetric assay and LC-MS/MS. The use of the colorimetric assay, the Arnow test, had the benefit of quickly providing information about what compounds resulted in catechol production. However, this method has several key caveats. Firstly, it is not possible to identify whether or not the catechol production observed comes directly from the consumption of the guaiacol because only a reading of total catechol produced is observed. In order to demonstrate that VMA and 3OMD are converted to their respective catechols, LC-MS/MS would need to be employed as was done to demonstrate the conversion of 2-ME<sub>2</sub> to 2-HE<sub>2</sub>. Secondly, the limit of detection for the Arnow test is significantly higher than more modern methods, with the range of limits of detection being between 20–60 μM depending on the catechol in question. This limited the ability to differentiate between how well bacterial species are able to metabolize specific guaiacols and requires high concentrations of guaiacols for *in vitro* incubations. While there is limited data on the concentration at which many guaiacols are present in the GI tract, modern assays (e.g., LC-MS/MS) have obtained limits of detection in the single-digit nanomolar range to accurately measure their catecholic precursors in serum and

stool. Ultimately, the use of LC–MS/MS will be important for future work in this project area to overcome these shortcomings.

The observed conversion of 2-ME<sub>2</sub> to 2-HE<sub>2</sub> suggests that additional metabolism may be occurring during *in vitro* incubations. By LC–MS/MS, we see that only a fraction of the total theoretical 2-HE<sub>2</sub> that could be produced by the provided 2-ME<sub>2</sub> is detected. A possible explanation is that additional metabolism is occurring. Dehydroxylation of 2-HE<sub>2</sub> was ruled out, as no estradiol was observed in samples. Another suspected outcome, though one that was not tested, was the oxidation of the alcohol at the 17-position, which would result in the formation of 2-hydroxyestrone. An untargeted mass spectrometry approach could provide additional information about the fate of unaccounted for 2-ME<sub>2</sub>.

## CONCLUSION

This work has identified additional guaiacols that the gut bacteria *E. limosum* and *B. producta* are capable of *O*-demethylating. One of these, 2-ME<sub>2</sub>, is definitively confirmed by LC–MS/MS, whereas the *O*-demethylation of VMA and 3OMD are suggested via the colorimetric Arnow test. This expands the known list of guaiacols from endogenous and pharmaceutical sources that are metabolized to their respective catechols by gut bacteria. By identifying the bacterial metabolizers at play in *O*-demethylation of guaiacols and the scope of guaiacols that can be acted upon, it allows for the study of particular metabolic activity *in vivo* to determine the impact of microbial metabolism on the host. Future experiments in germ-free mice will allow for the study of whether this *O*-demethylation occurs *in vivo*, allowing for an examination of the potential consequences for the health of the host.

## CHAPTER 3: Identifying Gut Bacterial Gene Required for Enterolactone Formation

The gut microbiome comprises hundreds of unique bacterial species residing in the gastrointestinal (GI) tract. These trillions of cells encode genes that allow gut bacteria to chemically modify molecules passing through the GI tract in ways that human cells cannot. This additional layer of chemical modifications represents a significant yet poorly understood source of individual variation in human metabolism with potentially profound impacts on health. For example, the gut microbiome is capable of converting plant-based dietary molecules into enterolactone (ENL),<sup>66</sup> a phytoestrogen with cancer-protective properties.<sup>67</sup> However, ENL production varies across individuals,<sup>68</sup> ENL is only produced through the enzymatic action of gut bacteria acting on polyphenolic precursor molecules,<sup>69</sup> called lignans, found in plant-based foods. The bioactivation of lignans to ENL was identified in the 1980s, but it was not until the 2000s that a consortium of gut bacteria capable of transforming one such lignan, secoisolariciresinol diglucoside (SDG), into ENL was identified.<sup>35</sup> However, the genetic basis for this metabolism was not identified. Indeed, many chemical transformations are associated with the gut microbiome, but the responsible species and genes are frequently unknown.<sup>6</sup> This poses a barrier to personalized, preventative medicine. Individual variation in gut microbiome composition means that ENL production also varies. Knowledge of the genes required for ENL biosynthesis from dietary lignan would enable the development of a genetically engineered probiotic that could impart this function to a non-ENL-producing individual. Such a probiotic, combined with a lignan-rich diet, could be used to reduce breast cancer risk.

Herein is identified a gut bacterial gene in *Lactonifactor longoviformis* that is sufficient for the bioactivation of END to ENL.<sup>28</sup> The transformation of END to ENL by *L. longoviformis* is the

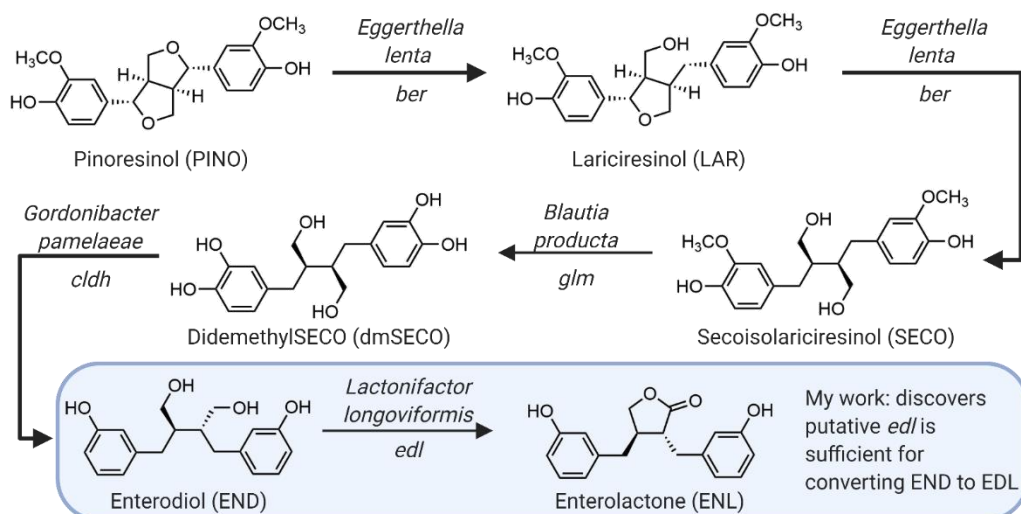


**Fig. 3.1** The lignan pinoresinol (PINO) is converted to the phytoestrogen enterolactone (ENL) by a consortium of gut bacteria. Recent work in the Bess and Turnbaugh Labs established a genetic mechanism for this pathway. I confirmed that *edl* is sufficient for the conversion of END to ENL.

last step of a series of reactions by a consortium of gut bacteria beginning with the dietary lignan pinoresinol (PINO) (**Fig 3.1**). *L. longoviformis* converts END to ENL through an oxidative cyclization—an unusual reaction in the reducing environment of the GI tract. Candidate genes in for the lactonization of END by *L. longoviformis* were identified by RNA sequencing. Under these conditions, two genes were substantially up-regulated: *edl1* (359.6-fold) and *edl2* (470.8-fold) (**Fig. S3**).<sup>28</sup> The sequences *edl1* and *edl2* correspond to a 4Fe-4S NADP-dependent oxidoreductase and a NAD(P)H-dependent short-chain dehydrogenase/reductase, respectively.<sup>28</sup> This, taken together with their inducible expression in the presence of END, suggested that *edl1* and *edl2* may be responsible for END lactonization; however, this had not been verified, nor had it been determined if both putative *edl* genes are required for metabolism or if either is sufficient. To test the hypothesized activity of these genes, a DNA construct was prepared and a liquid chromatography tandem mass spectrometry (LC–MS/MS) assay developed to assess the conversion of END to ENL by *edl1* and *edl2* heterologously expressed in *E. coli* Rosetta2 cells.

## MATERIALS AND METHODS

### Materials:

Enterodiol (END), enterolactone (ENL), secoisolariciresinol (SECO), and hydroxymatairesinol (HMR) were obtained from Separation Research (Turku, Finland). Ethyl acetate (+99.5% for

spectroscopy) used in extractions was purchased from Acros Organics. Acetonitrile (LiChrosolv®) and acetone (LiChrosolv®) used for LC–MS/MS sample preparation were purchased from Millipore Sigma.

#### Construction of Empty Vector:

A negative control vector (absent either *edI*) was prepared by excising *edI2* from the commercially synthesized pET151/D-TOPO-*edI2* plasmid. The V5 epitope and TEV restriction site of this plasmid were PCR amplified (forward primer: 5'-ATGCGCCATGGTAAGCCTATCCCTAAC-3'; reverse primer: 5'-GAGCTCATCGTGAATTCGTGAAGGGATCAATTCCTG-3'), introducing *NcoI* and *SacI* restriction sites with the forward and reverse primers, respectively. The resulting amplicon and pET151/D-TOPO-*edI2* were each digested with *NcoI* and *SacI* restriction enzymes (Thermo Fisher Scientific). Plasmid digestion excised the V5 epitope, TEV recognition site and *edI2*. Once the digested amplicon and plasmid fragments were ligated with T4 DNA ligase (New England Biolabs), a His-tag, V5 epitope and TEV restriction site (but no *edI2*) were maintained between the T7 promoter and T7 terminator. This plasmid (termed the empty vector) was introduced into *E. coli* Rosetta 2(DE3) cells.

#### Heterologous expression of EdI:

*E. coli* Rosetta 2 (DE3) cells with pET151/D-TOPO-*edI1*, pET151/D-TOPO-*edI2*, or empty vector or without (not transformed) and sterile controls were aerobically cultured at 37 °C overnight in lysogeny broth (LB). The resulting cultures were used to inoculate (1:100) lysogeny broth supplemented with 10 µM END (from a stock solution of 5 mM in DMSO) and µM isopropyl-β-D-thiogalactoside. Cultures were aerobically incubated at 48 h at 37 °C. The bacterial cells were then pelleted, and the supernatant harvested and immediately prepared for analysis by LC–MS/MS (described below). Prepared samples were analyzed immediately or frozen at -20 °C, thawed, and analyzed within 6 h of preparation.

### LC-MS/MS analysis of samples from EdI heterologous expression:

Concentrations of END and ENL from heterologous expression experiments were assessed by electrospray ionization (ESI) triple-quadrupole liquid chromatography mass spectrometry (Acquity UPLC and Quattro Premier XE; Waters Micromass) in negative-ion mode with single-reaction monitoring. Solvent A was 5 mM ammonium formate<sub>(aq)</sub>, while solvent B was 5% 5 mM ammonium formate<sub>(aq)</sub> and 95% acetonitrile. The concentration of solvent B was 40–95% from 0–4 min. The temperature was 50 °C. A C18 Column (Acquity UPLC BEH; 1.7 μM; 2.1 mm × 50 mm; Waters part number 186002350) was used. The injection volume was 10 μL. Retention times were as follows: END = 0.91 min; ENL = 0.67 min; and hydroxymatairesinol (HMR) = 0.62 min. The capillary voltage was 3.30 kV and the cone voltage was 10 V, with a source temperature of 125 °C. The desolvation gas flow was 800 L h<sup>-1</sup> and the desolvation temperature was 400 °C. The [M-H]<sup>-</sup>m/z values of parent/daughter ions were as follows: END = 301.08/252.90; ENL = 297.02/252.91; and HMR = 372.99/172.66. Stock solutions of END and ENL were prepared at 5 mM in DMSO. These were used to generate a standard containing END and ENL (each 20 μM in lysogeny broth), which was then serially diluted threefold to 3 nM. Each standard (125 μL) was diluted twofold into HMR (2 μM in double-distilled H<sub>2</sub>O). Standards were extracted with 0.5 mL ethyl acetate. The organic extracts were dried by centrifugal vacuum concentration (Refrigerated CentriVap Concentrator (Labconco part number 7310020) and DryFast Ultra (Welch part number 20422B-01)) and resuspended in 250 μL 25% acetone in water. The calibration curves used for quantification were 1.5 nM to 10 μM for END and 4.5 nM to 10 μM for ENL, with a limit of quantification set at a signal-to-noise ratio of 10:1. Calibration curves were generated by measuring peak areas and performing linear regression against known concentrations. Supernatant (50 μL) from incubations with END was diluted with 75 μL lysogeny broth and 125 μL HMR (2 μM in double-distilled H<sub>2</sub>O). Samples were extracted with 0.5 mL ethyl acetate. The organic extracts were dried by centrifugal vacuum concentration, resuspended in 250 μL 25%

acetone in water, and injected into the LC–MS/MS instrument. END and ENL concentrations were quantitated using calibration curves.

## RESULTS

To definitively assert that *edl1* or *edl2* is sufficient for *L. longoviformis* to metabolize END to ENL, heterologous expression of both of these genes was required, as well as two additional negative controls: incubations of END with the heterologous host and the heterologous host transformed with an empty vector. Heterologous expression was carried out using *edl1* and *edl2* cloned into separate pET151/D-TOPO vectors. This construct was prepared via DNA synthesis by Thermo Fisher, but the empty vector, a crucial negative control for verifying that the observed

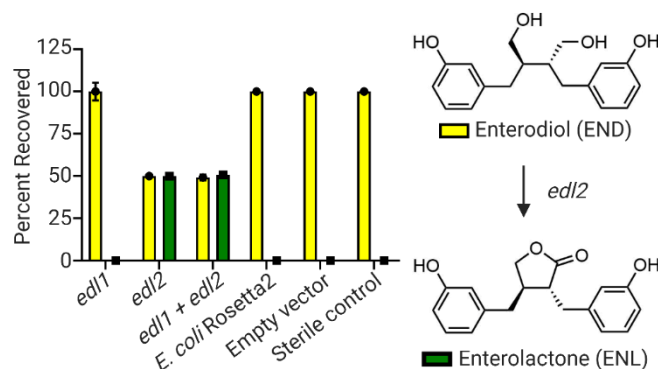


**Fig. 3.2** Percent conversion of enterodiol (END) to enterolactone (ENL) by LC–MS/MS (bars = mean  $\pm$  SEM, n = 3 biological replicates).

metabolism was only due to the gene of interest, was not commercially available. Consequently, the commercially prepared pET151/D-TOPO-*edl1* construct (**Fig. S4**) was used to reverse engineer the empty vector (**Fig. S5**). The empty vector was then transformed into *E. coli* Rosetta2 cells for use as a negative control.

Incubations with END were carried out with *E. coli* Rosetta 2 cells bearing either pET151/D-TOPO-*edl1* or pET151/D-TOPO-*edl2*. These two strains were also co-incubated, due to the possibility that both enzymes are required for metabolism. ENL was only detected in incubations with cells containing *edl2*, where approximately 50% of the recovered END had been converted to ENL (**Fig. 3.2**). The lack of conversion by *E. coli* Rosetta 2 bearing the empty vector confirms that the observed metabolism is due only to *edl2*. Incubations used racemic END, so observations that approximately 50% of END was converted to ENL is consistent with previous findings that *L. longoviformis* lactonizes (–)-ENL.<sup>8</sup> The same extent of conversion to ENL



measured upon incubation of END with Edl2-expressing cells was detected in the coincubation of bacteria encoding *edl1* and *edl2*, and no ENL was detected when the bacterium encoding *edl1* was incubated with END.

## DISCUSSION

Heterologous expression of *edl2* in *E. coli* resulted in conversion of END to ENL following *in vitro* incubation as assessed by LC–MS/MS, though heterologous expression of *edl1* did not. Together, these data suggest that *edl1*—neither alone nor in combination with *edl2*—does not encode conversion of END to ENL. Although heterologously expressed Edl1 was not sufficient for the conversion of END to ENL, it may still serve a purpose in ENL production in its native context. Testing this would require that *edl1* be knocked out in *L. longoviformis*, an organism for which genetic-engineering tools are currently lacking. Regardless, a responsible gene (*edl2*) has been identified in *L. longoviformis* for metabolism of END to ENL as a result of this work.

## CONCLUSION

Heterologous expression of two putative Edl enzymes confirms that *edl2* is sufficient for encoding conversion of END to ENL *in vitro*. The results of the full pathway by which gut bacteria convert PINO to ENL was recently published.<sup>28</sup> This new understanding of the genes underpinning ENL production by the gut microbiome opened the possibility of expressing this pathway heterologously in a probiotic. Such a probiotic combined with an intervening diet augment the metabolic capacity of one's gut microbiome to produce ENL from plant-based foods, thus potentially serving to decrease breast cancer risk. Should a successful probiotic be created, its *in vivo* efficacy can be tested in a mouse model in order to determine if colonization of an organism by the genetically engineered probiotic can increase enterolactone synthesis and circulation within a host.

## CHAPTER 4: Summary and Conclusions

The gut microbiome is known to be an important factor in human health and disease, yet the chemical mechanisms by which the gut microbiome exerts these impacts remain unknown. In each of these projects, chemical-level mechanisms by which the gut microbiome could have impacts on the host were explored. In the first, I proposed a novel method by which gut bacterial acetogens can produce dopamine. I identified two species, *E. limosum* and *B. producta*, which revert 3MT, a metabolite produced by human enzymes, to dopamine. This likely occurs via a cobalamin-dependent methyltransferase, as evinced by this metabolism being reversibly inhibited by propyl iodide. In the second, additional endogenous and pharmaceutical metabolites were found to be *O*-demethylated by these acetogens, including VMA, 3-OMD, and 2-ME<sub>2</sub>. Similar to 3MT, 2-ME<sub>2</sub> is produced by human COMT.<sup>51</sup> Both represent instances where gut bacterial metabolism counters a mechanism by which the body attenuates hormone levels. Therefore, their presence or absence has potential implications for the regulation of the hormones dopamine and estradiol in the host that merit further *in vivo* investigation. In the case of all of these guaiacols, it remains unknown what gene(s) are responsible for the observed metabolism. Understanding the bacterial genetics underlying this metabolism is crucial for a full understanding of how these gut bacteria may impact their host. Such work was undertaken in the third project to identify the gene in *L. longoviformis* responsible for converting the dietary metabolite END to the phytoestrogen ENL, which has been shown to have anticancer properties.<sup>66</sup> Each of these projects improves our understanding of the fundamental mechanisms by which the gut microbiome can impact the host. Future work on these projects in the Bess Lab will further this work by identifying these *in vivo* impacts in order to link these mechanisms to effects on the host. Ultimately, it is our hope that these explorations into the chemistry of the gut microbiome will build our understanding of how the gut microbiome impacts human health and disease.

## REFERENECS

1. Kinross, J. M.; Darzi, A. W; Nicholson, J. K. Gut Microbiome-Host Interactions in Health and Disease. *Genome Med.* **2011**, *3*. <https://doi.org/10.1186/gm228>
2. Kurilshikov, A.; Medina-Gomez, C.; Bacigalupe R. Large-Scale Association Analyses Identify Host Factors Influencing Human Gut Microbiome Composition. *Nat. Genet.* **2021**, *53*, 156–165. <https://doi.org/10.1038/s41588-020-00763-1>
3. Chiang, H.-L.; Lin, C-H. Altered Gut Microbiome and Intestinal Pathology in Parkinson's Disease. *J. Mov. Disord.* **2019**, *12*(2), 67–83. <https://doi.org/10.14802/jmd.18067>
4. Guinane, C.M.; Cotter, P.D. Role of the Gut Microbiota in Health and Chronic Gastrointestinal Disease: Understanding a Hidden Metabolic Organ. *Ther. Adv. Gastroenterol.* **2013**, *6*, 295–308. <https://doi.org/10.1177/1756283X13482996>
5. Fuhrman, B. J.; Feigelson, H. S.; Flores, R.; Gail, M. H.; Xu, X.; Ravel, J.; Goedert, J. J. Associations of the Fecal Microbiome with Urinary Estrogens and Estrogen Metabolites in Postmenopausal Women. *J. Clin. Endocrinol. Metab.* **2014**, *99* (12), 4632–4640.
6. Spanogiannopoulos, P.; Bess, E. N.; Carmody, R. N.; Turnbaugh, P. J. The Microbial Pharmacists Within: A Metagenomic View of Xenobiotic Metabolism. *Nat. Rev. Microbiol.* **2016**, *14*, 273–287.
7. Luczynski, P.; McVey Neufeld, K.-A.; Oriach, C. S.; Clarke, G.; Dinan, T. G.; Cryan, J. F. Growing up in a Bubble: Using Germ-Free Animals to Assess the Influence of the Gut Microbiota on Brain and Behavior. *Int. J. Neuropsychopharmacol.* **2016**, *19* (8). <https://doi.org/10.1093/ijnp/pyw020>.
8. Yano, J. M.; Yu, K.; Donaldson, G. P.; Shastri, G. G.; Ann, P.; Ma, L.; Nagler, C. R.; Ismagilov, R. F.; Mazmanian, S. K.; Hsiao, E. Y. Indigenous Bacteria from the Gut Microbiota Regulate Host Serotonin Biosynthesis. *Cell* **2015**, *161* (2), 264–276.
9. Reigstad, C. S.; Salmonson, C. E.; Rainey, J. F., 3rd; Szurszewski, J. H.; Linden, D. R.; Sonnenburg, J. L.; Farrugia, G.; Kashyap, P. C. Gut Microbes Promote Colonic Serotonin Production through an Effect of Short-Chain Fatty Acids on Enterochromaffin Cells. *FASEB J.* **2015**, *29* (4), 1395–1403.
10. Xue, R.; Zhang, H.; Pan, J.; Du, Z.; Zhou, W.; Zhang, Z.; Tian, Z.; Zhou, R.; Bai, L. Peripheral Dopamine Controlled by Gut Microbes Inhibits Invariant Natural Killer T Cell-Mediated Hepatitis. *Front. Immunol.* **2018**, *9*, 2398.
11. Cryan, J. F.; Dinan, T. G. Mind-Altering Microorganisms: The Impact of the Gut Microbiota on Brain and Behaviour. *Nat. Rev. Neurosci.* **2012**, *13* (10), 701–712.
12. Galland, L. The Gut Microbiome and the Brain. *J. Med. Food* **2014**, *17* (12), 1261–1272.
13. Barbeau, A.; Murphy, G. F.; Sourkes, T. L. Excretion of Dopamine in Diseases of Basal Ganglia. *Science* **1961**, *133* (3465), 1706–1707.
14. Goldstein, D. S.; Swoboda, K. J.; Miles, J. M.; Coppack, S. W.; Aneman, A.; Holmes, C.; Lamensdorf, I.; Eisenhofer, G. Sources and Physiological Significance of Plasma Dopamine Sulfate. *J. Clin. Endocrinol. Metab.* **1999**, *84* (7), 2523–2531.
15. Eisenhofer, G.; Aneman, A.; Friberg, P.; Hooper, D.; Fändriks, L.; Lonroth, H.; Hunyady, B.; Mezey, E. Substantial Production of Dopamine in the Human Gastrointestinal Tract. *J. Clin. Endocrinol. Metab.* **1997**, *82* (11), 3864–3871.
16. Asano, Y.; Hiramoto, T.; Nishino, R.; Aiba, Y.; Kimura, T.; Yoshihara, K.; Koga, Y.; Sudo, N. Critical Role of Gut Microbiota in the Production of Biologically Active, Free Catecholamines in the Gut Lumen of Mice. *Am. J. Physiol. Gastrointest. Liver Physiol.* **2012**, *303* (11), G1288–G1295.
17. Martin, G.; Forte, P.; Luchsinger, A.; Mendoza, F.; Urbina-Quintana, A.; Hernandez Pieretti, O.; Romero, E.; Velasco, M. Dopamine-Induced Antihypertensive Effects and Plasma Insulin Rise Are Blocked by Metoclopramide in Labetalol-Treated Patients. *J.*

- Clin. Pharmacol.* **1994**, *34* (1), 91–94.
18. Rubí, B.; Maechler, P. Minireview: New Roles for Peripheral Dopamine on Metabolic Control and Tumor Growth: Let's Seek the Balance. *Endocrinology* **2010**, *151* (12), 5570–5581.
  19. Ben-Jonathan; Nira. *Dopamine : Endocrine and Oncogenic Functions*; 2020.
  20. Sonne, J.; Goyal, A.; Bansal, P.; Lopez-Ojeda, W. Dopamine. In *StatPearls*; StatPearls Publishing: Treasure Island (FL), 2021.
  21. Maini Rekdal, V.; Bess, E. N.; Bisanz, J. E.; Turnbaugh, P. J.; Balskus, E. P. Discovery and Inhibition of an Interspecies Gut Bacterial Pathway for Levodopa Metabolism. *Science* **2019**, *364* (6445). <https://doi.org/10.1126/science.aau6323>.
  22. van Kessel, S. P.; Frye, A. K.; El-Gendy, A. O.; Castejon, M.; Keshavarzian, A.; van Dijk, G.; El Aidy, S. Gut Bacterial Tyrosine Decarboxylases Restrict Levels of Levodopa in the Treatment of Parkinson's Disease. *Nat. Commun.* **2019**, *10* (1), 310.
  23. Valles-Colomer, M.; Falony, G.; Darzi, Y.; Tigchelaar, E. F.; Wang, J.; Tito, R. Y.; Schiweck, C.; Kurilshikov, A.; Joossens, M.; Wijmenga, C.; Claes, S.; Van Oudenhove, L.; Zhernakova, A.; Vieira-Silva, S.; Raes, J. The Neuroactive Potential of the Human Gut Microbiota in Quality of Life and Depression. *Nat. Microbiol.* **2019**, *4* (4), 623–632.
  24. Itäaho, K.; Court, M. H.; Uutela, P.; Kostianen, R.; Radomska-Pandya, A.; Finel, M. Dopamine Is a Low-Affinity and High-Specificity Substrate for the Human UDP-Glucuronosyltransferase 1A10. *Drug Metab. Dispos.* **2009**, *37* (4), 768–775.
  25. Wang, Y.; Tong, Q.; Ma, S.-R.; Zhao, Z.-X.; Pan, L.-B.; Cong, L.; Han, P.; Peng, R.; Yu, H.; Lin, Y.; Gao, T.-L.; Shou, J.-W.; Li, X.-Y.; Zhang, X.-F.; Zhang, Z.-W.; Fu, J.; Wen, B.-Y.; Yu, J.-B.; Cao, X.; Jiang, J.-D. Oral Berberine Improves Brain Dopa/dopamine Levels to Ameliorate Parkinson's Disease by Regulating Gut Microbiota. *Signal Transduct. Target Ther.* **2021**, *6* (1), 77.
  26. Axelrod, J.; Tomchick, R. Enzymatic O-Methylation of Epinephrine and Other Catechols. *J. Biol. Chem.* **1958**, *233* (3), 702–705.
  27. Uhlén, M.; Fagerberg, L.; Hallström, B. M.; Lindskog, C.; Oksvold, P.; Mardinoglu, A.; Sivertsson, Å.; Kampf, C.; Sjöstedt, E.; Asplund, A.; Olsson, I.; Edlund, K.; Lundberg, E.; Navani, S.; Szgyarto, C. A.-K.; Odeberg, J.; Djureinovic, D.; Takanen, J. O.; Hober, S.; Alm, T.; Edqvist, P.-H.; Berling, H.; Tegel, H.; Mulder, J.; Rockberg, J.; Nilsson, P.; Schwenk, J. M.; Hamsten, M.; von Feilitzen, K.; Forsberg, M.; Persson, L.; Johansson, F.; Zwahlen, M.; von Heijne, G.; Nielsen, J.; Pontén, F. Proteomics. Tissue-Based Map of the Human Proteome. *Science* **2015**, *347* (6220), 1260419.
  28. Bess, E. N.; Bisanz, J. E.; Yarza, F.; Bustion, A.; Rich, B. E.; Li, X.; Kitamura, S.; Waligurski, E.; Ang, Q. Y.; Alba, D. L.; Spanogiannopoulos, P.; Nayfach, S.; Koliwad, S. K.; Wolan, D. W.; Franke, A. A.; Turnbaugh, P. J. Genetic Basis for the Cooperative Bioactivation of Plant Lignans by *Eggerthella lenta* and Other Human Gut Bacteria. *Nat. Microbiol.* **2020**, *5* (1), 56–66.
  29. Sharak Genthner, B. R.; Bryant, M. P. Additional Characteristics of One-Carbon-Compound Utilization by *Eubacterium limosum* and *Acetobacterium woodii*. *Appl. Environ. Microbiol.* **1987**, *53* (3), 471–476.
  30. Misoph, M.; Daniel, S. L.; Drake, H. L. Bidirectional Usage of Ferulate by the Acetogen *Peptostreptococcus Productus* U-1: CO<sub>2</sub> and Aromatic Acrylate Groups as Competing Electron Acceptors. *Microbiology* **1996**, *142* (8), 1983–1988.
  31. Clavel, T.; Borrmann, D.; Braune, A.; Doré, J.; Blaut, M. Occurrence and Activity of Human Intestinal Bacteria Involved in the Conversion of Dietary Lignans. *Anaerobe* **2006**, *12* (3), 140–147.
  32. Rivera-Calimlim, L. Absorption, Metabolism and Distribution of (14C)-O-Methyldopa and (14C)-L-Dopa after Oral Administration to Rats. *Br. J. Pharmacol.* **1974**, *50* (2), 259–263.
  33. Jianguo, L.; Xueyang, J.; Cui, W.; Changxin, W.; Xuemei, Q. Altered Gut Metabolome

- Contributes to Depression-like Behaviors in Rats Exposed to Chronic Unpredictable Mild Stress. *Transl. Psychiatry* **2019**, *9* (1), 1–14.
34. Ma, S.-R.; Yu, J.-B.; Fu, J.; Pan, L.-B.; Yu, H.; Han, P.; Zhang, Z.-W.; Peng, R.; Xu, H.; Wang, Y. Determination and Application of Nineteen Monoamines in the Gut Microbiota Targeting Phenylalanine, Tryptophan, and Glutamic Acid Metabolic Pathways. *Molecules* **2021**, *26* (5). <https://doi.org/10.3390/molecules26051377>.
  35. Clavel, T.; Henderson, G.; Engst, W.; Doré, J.; Blaut, M. Phylogeny of Human Intestinal Bacteria That Activate the Dietary Lignan Secoisolariciresinol Diglucoside. *FEMS Microbiol. Ecol.* **2006**, *55* (3), 471–478.
  36. Bache, R.; Pfennig, N. Selective Isolation of *Acetobacterium woodii* on Methoxylated Aromatic Acids and Determination of Growth Yields. *Arch. Microbiol.* **1981**, *130* (3), 255–261.
  37. Frazer, A. C.; Young, L. Y. A Gram-Negative Anaerobic Bacterium That Utilizes O-Methyl Substituents of Aromatic Acids. *Appl. Environ. Microbiol.* **1985**, *49* (5), 1345–1347.
  38. Frazer Anne Cornish; Young L. Y. Anaerobic C1 Metabolism of the O-Methyl-<sup>14</sup>C-Labeled Substituent of Vanillate. *Appl. Environ. Microbiol.* **1986**, *51* (1), 84–87.
  39. Naidu Devendra; Ragsdale Stephen W. Characterization of a Three-Component Vanillate O-Demethylase from *Moorella thermoacetica*. *J. Bacteriol.* **2001**, *183* (11), 3276–3281.
  40. Coccagn, M.; Wilberg, E.; Lindley, N. D. Sequential Demethoxylation Reactions during Methylotrophic Growth of Methoxylated Aromatic Substrates with *Eubacterium limosum*. *Arch. Microbiol.* **1991**, *155* (5), 496–499.
  41. Wang, L.-Q.; Meselhy, M. R.; Li, Y.; Qin, G.-W.; Hattori, M. Human Intestinal Bacteria Capable of Transforming Secoisolariciresinol Diglucoside to Mammalian Lignans, Enterodiols and Enterolactone. *Chem. Pharm. Bull.* **2000**, *48* (11), 1606–1610.
  42. Possemiers, S.; Rabot, S.; Espín, J. C.; Bruneau, A.; Philippe, C.; González-Sarrías, A.; Heyerick, A.; Tomás-Barberán, F. A.; De Keukeleire, D.; Verstraete, W. *Eubacterium Limosum* Activates Isoxanthohumol from Hops (*Humulus Lupulus L.*) into the Potent Phytoestrogen 8-Prenylnaringenin *in Vitro* and in Rat Intestine. *J. Nutr.* **2008**, *138* (7), 1310–1316.
  43. Burapan, S.; Kim, M.; Han, J. Demethylation of Polymethoxyflavones by Human Gut Bacterium, *Blautia* Sp. MRG-PMF1. *J. Agric. Food Chem.* **2017**, *65* (8), 1620–1629.
  44. Schilhabel, A.; Studenik, S.; Vödisch, M.; Kreher, S.; Schlott, B.; Pierik, A. J.; Diekert, G. The Ether-Cleaving Methyltransferase System of the Strict Anaerobe *Acetobacterium Dehalogenans*: Analysis and Expression of the Encoding Genes. *J. Bacteriol.* **2009**, *191* (2), 588–599.
  45. Kelly, W. J.; Henderson, G.; Pacheco, D. M.; Li, D.; Reilly, K.; Naylor, G. E.; Janssen, P. H.; Attwood, G. T.; Altermann, E.; Leahy, S. C. The Complete Genome Sequence of *Eubacterium Limosum* SA11, a Metabolically Versatile Rumen Acetogen. *Stand. Genomic Sci.* **2016**, *11*, 26.
  46. Kage, S.; Kudo, K.; Ikeda, H.; Ikeda, N. Simultaneous Determination of Formate and Acetate in Whole Blood and Urine from Humans Using Gas Chromatography-Mass Spectrometry. *J. Chromatogr. B Analyt. Technol. Biomed. Life Sci.* **2004**, *805* (1), 113–117.
  47. Maini Rekdal, V.; Nol Bernadino, P.; Luescher, M. U.; Kiamehr, S.; Le, C.; Bisanz, J. E.; Turnbaugh, P. J.; Bess, E. N.; Balskus, E. P. A Widely Distributed Metalloenzyme Class Enables Gut Microbial Metabolism of Host- and Diet-Derived Catechols. *Elife* **2020**, *9*. <https://doi.org/10.7554/eLife.50845>.
  48. Berman, M. H.; Frazer, A. C. Importance of Tetrahydrofolate and ATP in the Anaerobic O-Demethylation Reaction for Phenylmethylethers. *Appl. Environ. Microbiol.* **1992**, *58*

- (3), 925–931.
49. Brot, N.; Weissbach, H. Enzymatic Synthesis of Methionine. Chemical Alkylation of the Enzyme-Bound Cobamide. *J. Biol. Chem.* **1965**, *240*, 3064–3070.
  50. Groher, A.; Weuster-Botz, D. General Medium for the Autotrophic Cultivation of Acetogens. *Bioprocess Biosyst. Eng.* **2016**, *39* (10), 1645–1650.
  51. Männistö, P. T.; Kaakkola, S. Catechol-O-Methyltransferase (COMT): Biochemistry, Molecular Biology, Pharmacology, and Clinical Efficacy of the New Selective COMT Inhibitors. *Pharmacol. Rev.* **1999**, *51* (4), 593–628.
  52. Hur, H.-G.; Rafii, F. Biotransformation of the Isoflavonoids Biochanin A, Formononetin, and Glycitein by *Eubacterium Limosum*. *FEMS Microbiol. Lett.* **2000**, *192* (1), 21–25.
  53. Chen, J.-X.; Deng, C.-Y.; Zhang, Y.-T.; Liu, Z.-M.; Wang, P.-Z.; Liu, S.-L.; Qian, W.; Yang, D.-H. Cloning, Expression, and Characterization of a Four-Component O-Demethylase from Human Intestinal Bacterium *Eubacterium limosum* ZL-II. *Appl. Microbiol. Biotechnol.* **2016**, *100* (21), 9111–9124.
  54. Ghambeer, R. K.; Wood, H. G.; Schulman, M.; Ljungdahl, L. Total Synthesis of Acetate from CO<sub>2</sub>. 3. Inhibition by Alkylhalides of the Synthesis from CO<sub>2</sub>, Methyltetrahydrofolate, and Methyl-B12 by *Clostridium thermoaceticum*. *Arch. Biochem. Biophys.* **1971**, *143* (2), 471–484.
  55. Matthews, R. G.; Koutmos, M.; Datta, S. Cobalamin-Dependent and Cobamide-Dependent Methyltransferases. *Curr. Opin. Struct. Biol.* **2008**, *18* (6), 658–666.
  56. Chang, I. S.; Kim, B. H.; Kim, D. H.; Lovitt, R. W.; Sung, H. C. Formulation of Defined Media for Carbon Monoxide Fermentation by *Eubacterium limosum* KIST612 and the Growth Characteristics of the Bacterium. *J. Biosci. Bioeng.* **1999**, *88* (6), 682–685.
  57. Geerligs, G.; Aldrich, H. C.; Harder, W.; Diekert, G. Isolation and Characterization of a Carbon Monoxide Utilizing Strain of the Acetogen *Peptostreptococcus Productus*. *Arch. Microbiol.* **1987**, *148* (4), 305–313.
  58. Høverstad, T.; Midtvedt, T. Short-Chain Fatty Acids in Germfree Mice and Rats. *J. Nutr.* **1986**, *116* (9), 1772–1776.
  59. Miller, T. L.; Wolin, M. J. Pathways of Acetate, Propionate, and Butyrate Formation by the Human Fecal Microbial Flora. *Appl. Environ. Microbiol.* **1996**, *62* (5), 1589–1592.
  60. Barker, H. A.; Kamen, M. D. Carbon Dioxide Utilization in the Synthesis of Acetic Acid by *Clostridium Thermoaceticum*. *Proc. Natl. Acad. Sci. U. S. A.* **1945**, *31* (8), 219–225.
  61. Wood, H. G. A Study of Carbon Dioxide Fixation by Mass Determination of the Types of C<sup>13</sup>-Acetate. *J. Biol. Chem.* **1952**, *194* (2), 905–931.
  62. Ljungdahl, L.; Irion, E.; Wood, H. G. Total Synthesis of Acetate from CO<sub>2</sub>. I. Co-Methylcobyric Acid and CO-(methyl)-5-Methoxybenzimidazolylcobamide as Intermediates with *Clostridium thermoaceticum*. *Biochemistry* **1965**, *4* (12), 2771–2780.
  63. Haskel, Y.; Hanani, M. Inhibition of Gastrointestinal Motility by MPTP via Adrenergic and Dopaminergic Mechanisms. *Dig. Dis. Sci.* **1994**, *39* (11), 2364–2367.
  64. Arnow, L. E. Colorimetric determination of the components of 3,4-dihydroxyphenylalaninetyrosine mixtures. *J. Biol. Chem.* **1937**, *118*, 531–537.
  65. Fuhrman, B. J.; Schairer, C.; Gail, M. H.; Boyd-Morin, J.; Xu, X.; Sue, L.Y.; Buys, S. S.; Isaacs, C.; Keefer, L. K.; Veenstra, T. D.; Berg, C. D.; Hoover, R. N.; Ziegler, R. G. Estrogen metabolism and risk of breast cancer in postmenopausal women. *JNCI* **2012**, *104*(4), 326–339.
  66. Borriello, S. P.; Setchell, K. D.; Axelson, M.; Lawson, A. M. Production and metabolism of lignans by the human faecal flora. *J. Appl. Bacteriol.* **1985**, *58*, 37–43.
  67. Mabrok, H. B.; Klopffleisch, R.; Ghanem, K. Z.; Clavel, T.; Blaut, M.; Loh, G. Lignan transformation by gut bacteria lowers tumor burden in a gnotobiotic rat model of breast cancer. *Carcinogenesis.* **2012**, *33*(1), 203–208.

68. Halldin, E.; Eriksen, A. K.; Brunius, C.; da Silva, A. B.; Bronze, M.; Hanhineva, K.; Aura, A.-M.; Landberd, R. Factors explaining interpersonal variation in plasma enterolactone concentration in humans. *Mol. Nutr. Food Res.* **2019**, *63*, 1801159.
69. Woting, A.; Clavel, T.; Loh, G.; Blaut, M. Bacterial transformation of dietary lignans in gnotobiotic rats. *FEMS Microbiol. Ecol.* **2010**, *72*(3), 507–514.

## APPENDIX A

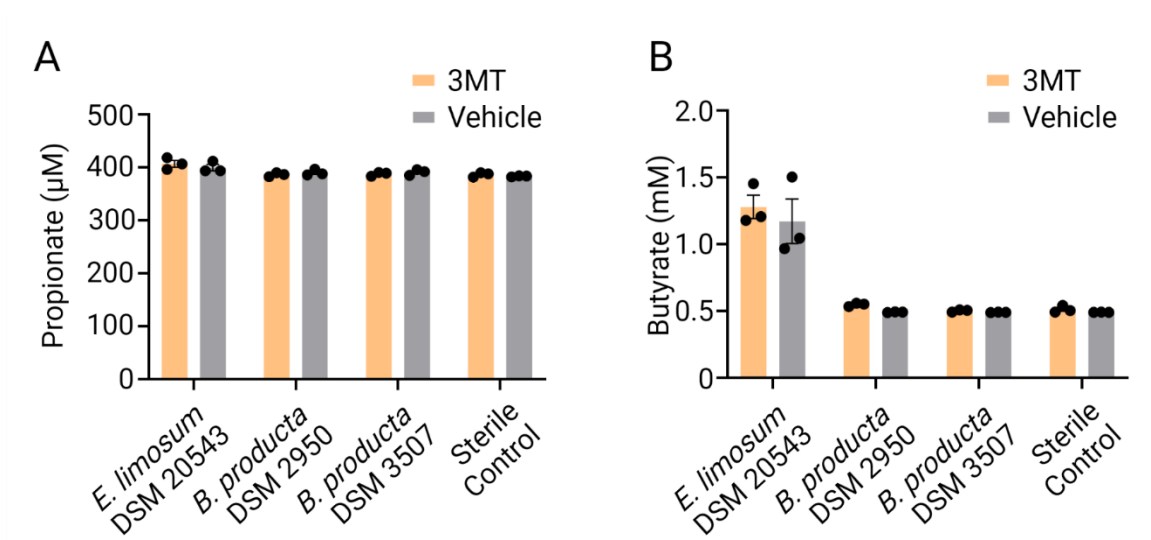


**Fig. S2.** *E. limosum* DSM 20543 and *B. producta* strains DSM 2950 and DSM 3507 were each cultured using acetogenic media with 3MT (2 mM) or vehicle. **(A)** Propionate and **(B)** butyrate levels were assessed by GC–MS. (n = 3 biological replicates; bars are mean ± SEM).

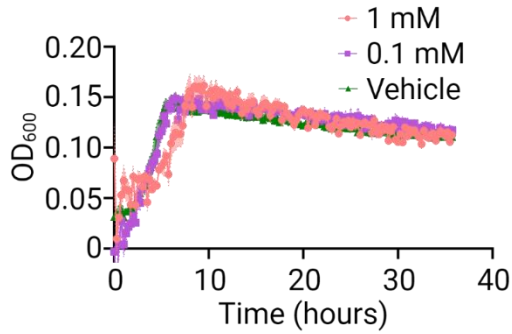


**Fig. S2.** *B. producta* DSM 3507 was cultured in acetogenic media with varying concentrations of 3MT (1 mM, 0.1 mM) or vehicle to assess differences in growth via OD<sub>600</sub> (n = 3 biological replicates; values are mean ± SEM).



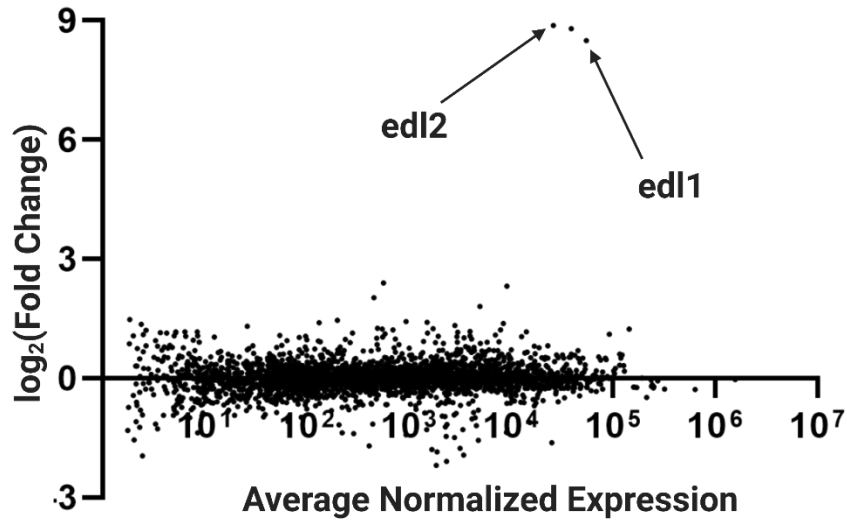


**Fig. S3** RNA sequencing was used to identify the relative upregulation of genes in the presence of END. Three such genes were substantially upregulated. Two of those were identified as *edl1* and *edl2*. The third gene was seen as unlikely to be the responsible gene as its sequence bears the greatest similarity to MFS transporters.<sup>28</sup>

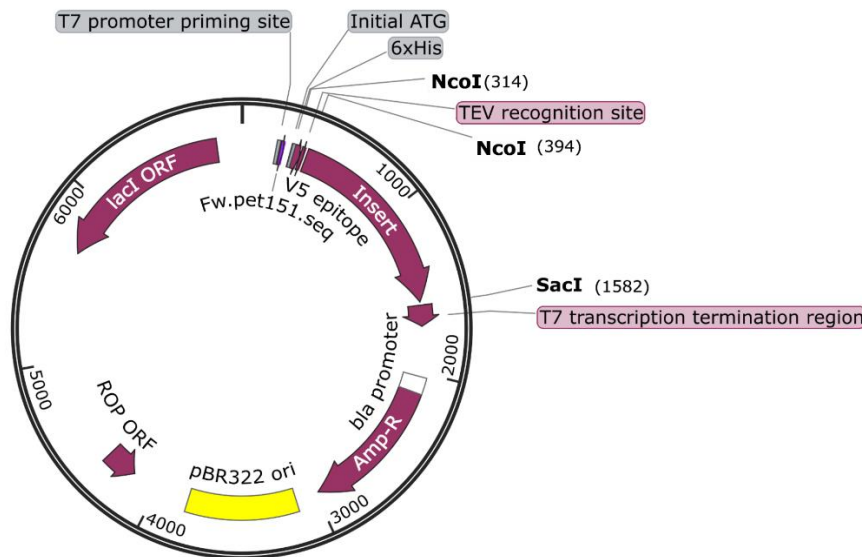


**Fig. S4** Plasmid map for pET151/D-TOPO\_ *edl1*, where *edl1* is represented as “Insert”. NcoI and SacI restriction enzymes were used to excise the insert en route to the negative control vector. This excision also removed the V5 epitope and TEV binding region. See sequencing in Supp. Table 1.

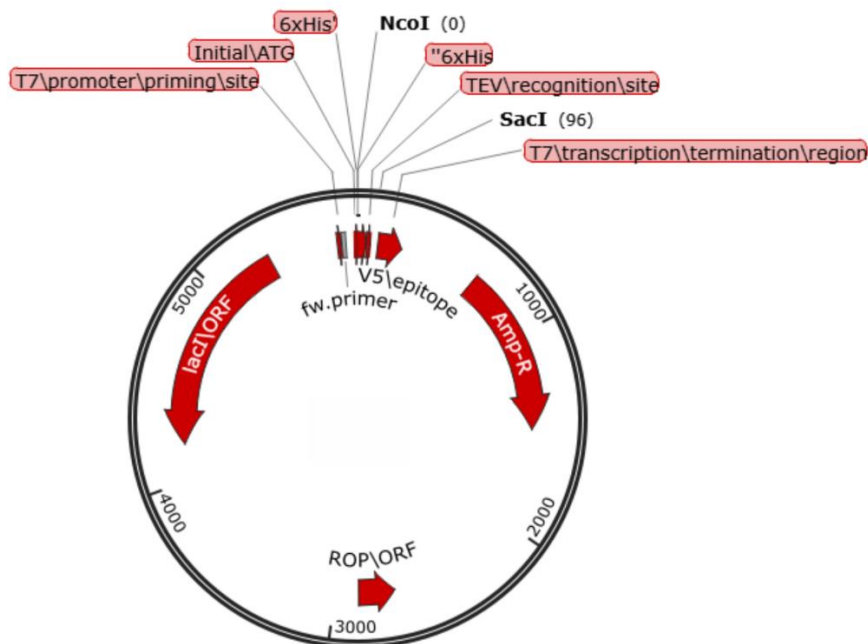


**Fig. S4** The region containing the V5 epitope and TEV binding region from the plasmid in Supplemental Fig. 2 was amplified and ligated into the digested plasmid to create an empty vector that has all of the features as pET/D-TOPO\_ed1, including the V5 epitope and TEV binding region, except for the insert. See **Table S1** for sequencing.

**Table S1** To verify that the insert was removed, the region between the V5 epitope and T7 transcription termination site (see Supp. Fig. 2 and Supp. Fig. 3) was amplified by PCR (Forward primer: GTGAGCGGATAACAATTCCC; Reverse primer: CAAGACCCGTTTAGAGGC) and Sanger sequenced. In pET151/D-TOPO\_ed1, the insert *ed1* (is still present whereas it has been removed in the empty vector as confirmed by Sanger sequencing.

Plasmid	Sequence amplified between V5 epitope and T7 transcription termination region
pET151/D - TOPO_ed 11	GGTAAGCCTATCCCTAACCTCTCCTCGGTCTCGATTCTACGGAAAACCTG TATTTTCAGGGAATTGATCCCTTACCCATGGCCATCAATTTTGGTAAACGCT TTGGTTTAGGTGGTCTGCGTCTGCCGATTAGCGATCCGAATGAACAGCGTA GCATTGATTATGAAACCCTGGAAAACATGATCGATATCTTTATGGATCACGG CTTCAACTATTTGATACCAGCTATATCTATCACGGTGGCTTTAGCGAAATT GCACTGGGTAAAGCACTGGTTGATCGTTATCCGCGTGATAGCTTTCTGCTG AGCACCAAATGCCGATCAAATTCATGAAAAGAAAGAAGATATGGAAACCA TCTTTGAAGAACAGCTGGAAAATGCCACGTGGATTACTTTGATTTCTATCT GATTCACAGCATCGGCAAAGAAACCTATGAGAACTGTAAAAAATGGGATAC CTTCGAGTTCCTGAAACAGAAACGTGCCGAAGGTAAATTTCTGTAATTTGGT GTTAGCCTGCATGACAGTCCGGAATTTCTGGATCTGATTCTGACCGAACAT CCGGAATTGATTTTGTGATTGAGCAGATCAACTACATCGATTGGGAAAATC CGGCAATTCGCAGCAAAGAAATTTATGAAGTTGCCGTGAAACATGGCAAAC CGATTGTTGTTATGGAAGCATGTAAAGGTGGCACCCCTGGCCGAAGTTCCGG ATGAAGCCAAAAAATCATGAAAGAATATAACCCGGATGCCAGCATTGCCA GCTGGGCATATCGTTTTGTTGGTAGCCTGCCTGGTGTTCGTGTTGTTCTGG CAGGTATGCCTCGTATGGAATTCCTGTATGATAACATCAAACCTTTGAAGA GTTTCAGCCGCTGAACGAAGAAGAGTATAAAATCATTGACAAAGTGGTGGA

	AATCATCAATGCGAATACCCCGATTCCGTGTACCGTTTGTGCGTTATTGTGAA AGCGAATGCCCGAAAAACATTGCCATTCCGGATTATTTTGCCCTGTACAATG ATATGAAGCGTCTGGAAAAAAGCAGCAGCGCAAATGATGTTCTGACCCAGG CATTCTATTATGGCAACTTTATTGAACAAGGTCTGTGGTCCGGCAAGCGCAT GTATTAATGTGAAAAATGCGTTAAAGTGTGTCCGCAGCGCCTGGAAATTC CGAAATATCTGGAAGAATATGTTGTGGCAGAAGCTGAAAGCTATAATCCTGA AGCACAGATCAAGAAATAAAAGGGCGAGCTCAGATCCGGCTGCTAACAAAG CCCGAAAGGAAGCTGAGTTGGCTGCTGCCACCGCTGAGCAATAACTAGCA TAACCCCTTGGGGCCTCTAAACGGGTC
Empty Vector	GAGATATACATATGCATCATCACCATCACCATGGTAAGCCTATCCCTAACCC TCTCCTCGGTCTCGATTCTACGGAAAACCTGTATTTTCAGGGAATTGATCCC TTCACGAATTCACGATGAGCTCAGATCCGGCTGCTAACAAAGCCCGAAAGG AAGCTGAGTTGGCTGCTGCCACCGCTGAGC
<i>edl</i> insert	ATGGCCATCAATTTTGGTAAACGCTTTGGTTTAGGTGGTCTGCGTCTGCCG ATTAGCGATCCGAATGAACAGCGTAGCATTGATTATGAAACCCTGGAAAAC ATGATCGATATCTTTATGGATCACGGCTTCAACTATTTTCGATACCAGCTATAT CTATCACGGTGGCTTTAGCGAAATTGCACTGGGTAAAGCACTGGTTGATCG TTATCCGCGTGATAGCTTTCTGCTGAGCACCAAATGCCGATCAAATTCATG AAAAAGAAAGAAGATATGGAAACCATCTTTGAAGAACAGCTGGAAAAATGC CACGTGGATTACTTTGATTTCTATCTGATTCACAGCATCGGCAAAGAAACCT ATGAGAAGTGTAAAAATGGGATACCTTCGAGTTCCTGAAACAGAAACGTG CCGAAGGTAAATTTTCGTGAATTTGGTGTAGCCTGCATGACAGTCCGGAAT TTCTGGATCTGATTCTGACCGAACATCCGGAAATTGATTTTGTGATTGAGCA GATCAACTACATCGATTGGGAAAATCCGGCAATTCGCAGCAAAGAAATTTAT GAAGTTGCCGTGAAACATGGCAAACCGATTGTTGTTATGGAAGCATGTAAA GGTGGCACCCCTGGCCGAAGTTCCGGATGAAGCCAAAAAATCATGAAAGAA TATAACCCGGATGCCAGCATTGCCAGCTGGGCATATCGTTTTGTTGGTAGC CTGCCTGGTGTTCGTGTTGTTCTGGCAGGTATGCCTCGTATGGAATTCCTG TATGATAACATCAAAACCTTTGAAGAGTTTCAGCCGCTGAACGAAGAAGAGT ATAAAATCATTGACAAAGTGGTGGAAATCATCAATGCGAATACCCCGATTCC GTGTACCGTTTGTGCGTTATTGTGAAAGCGAATGCCCGAAAAACATTGCCATT CCGATTATTTTGCCCTGTACAATGATATGAAGCGTCTGGAAAAAAGCAGC AGCGCAAATGATGTTCTGACCCAGGCATTCTATTATGGCAACTTTATTGAAC AAGGTCGTGGTCCGGCAAGCGCATGTATTAATGTGAAAAATGCGTTAAAG TGTGTCCGCAGCGCCTGGAAATTCGAAATATCTGGAAGAATATGTTGTGG CAGAAGTGGAAAGCTATAATCCTGAAGCACAGATCAAGAAATAA